NACA

RESEARCH MEMORANDUM

THE EFFECT OF WING FENCES ON THE LONGITUDINAL CHARACTERISTICS AT MACH NUMBERS UP TO 0.92 OF A WING-FUSELAGE-TAIL COMBINATION HAVING A 40° SWEPTBACK WING WITH NACA 64A THICKNESS DISTRIBUTION

By Jerald K. Dickson and Fred B. Sutton

Ames Aeronautical Laboratory
Moffett Field, Calif.

NATIONAL ADVISORY COMMITTEE
FOR AERONAUTICS

WASHINGTON

May 27, 1955

NATIONAL ADVISORY COMMITTEE FOR AERONAUTICS

RESEARCH MEMORANDUM

THE EFFECT OF WING FENCES ON THE LONGITUDINAL CHARACTERISTICS AT MACH NUMBERS UP TO 0.92 OF A WING-FUSELAGE-TAIL COMBINATION HAVING A 40° SWEPTBACK WING WITH NACA 64A THICKNESS DISTRIBUTION

By Jerald K. Dickson and Fred B. Sutton

SUMMARY

A wind-tunnel investigation has been conducted to determine the effects of various wing-fence arrangements upon the longitudinal characteristics of a wing-fuselage and wing-fuselage-tail combination having a wing with 40° of sweepback, an aspect ratio of 7.0, and NACA 64A thickness distribution. The tests were made through an angle-of-attack range at a Mach number of 0.25 and a Reynolds number of 8 million, and at Mach numbers varying from 0.25 to 0.92 at a Reynolds number of 2 million.

The addition of multiple wing fences to the wing-fuselage and wing-fuselage-tail combination eliminated large changes in longitudinal stability to lift coefficients in excess of 1.0 at a Mach number of 0.25 and a Reynolds number of 8 million, an improvement of as much as 50 percent over the values with the fences off. At high subcritical and supercritical speeds, these large changes in stability occurred at lift coefficients near 0.60 without fences and at lift coefficients between 0.70 and 0.80 with fences. The addition of fences increased the drag moderately at low lift coefficients, but usually reduced the drag and increased the lift-drag ratios at the higher lift coefficients. The Mach numbers for drag divergence were increased slightly by the addition of fences; however, the corresponding drag coefficients were higher than those corresponding to the divergence Mach numbers without fences.

The fences had only small effect on the contribution of the horizontal tail to the longitudinal stability at low speed and high Reynolds number, and at moderate lift coefficients and high speeds. The all-movable tail had nearly constant control effectiveness throughout the lift range at most Mach numbers, and its effectiveness as a longitudinal control at an angle of attack of 4° was usually increased moderately by increasing Mach number.

INTRODUCTION

The longitudinal characteristics of wings suitable for long-range airplanes capable of high subsonic speeds have been the subject of an investigation in the Ames 12-foot pressure wind tunnel. Two twisted and cambered wings of relatively high aspect ratio, one having NACA four-digit and the other having NACA 64A thickness distribution, have been investigated at 40°, 45°, and 50° of sweepback. These results are presented in reference 1. All of these wings experienced a severe decrease in longitudinal stability at moderate lift coefficients due to the onset of stalling over the outer portions of the span. The results in reference 2 show that the stability characteristics of the wings having NACA four-digit thickness distribution could be improved considerably by the use of chordwise fences.

The present phase of the investigation was directed toward the development of wing fences which would improve the longitudinal stability characteristics of the wing with NACA 64A thickness distribution. The wing was tested at 40° of sweepback with a fuselage and various fence arrangements. The fences were systematically varied in spanwise position, number, and chordwise extent to establish the fence configuration which afforded the greatest improvement in stability. The results obtained with the best of these fences are compared with the results of the investigation reported in reference 2. The wing-fuselage combination with and without the most satisfactory fences was also tested with an all-movable horizontal tail at two angles of incidence to determine the effect of the wing fences on the tail contribution to stability and the control effectiveness of the tail.

NOTATION

A	aspect ratio, $\frac{b^2}{2S}$
a	mean-line designation, fraction of chord over which design load is uniform
a_t	lift-curve slope of the isolated horizontal tail, per deg
a_{w+f}	lift-curve slope of the wing-fuselage combination, per deg
a_{w+f+t}	lift-curve slope of the wing-fuselage-tail combination, per deg
$\frac{b}{2}$	wing semispan perpendicular to the plane of symmetry
C_D	drag coefficient, $\frac{\text{drag}}{qS}$

C_L lift coefficient, $\frac{\text{lift}}{qS}$

C_{L_i} inflection lift coefficient, lowest positive lift coefficient at which $\frac{dC_m}{dC_L} = 0$

C_m pitching-moment coefficient about the quarter point of the wing mean aerodynamic chord, $\frac{\text{pitching moment}}{qS\bar{c}}$

c local chord parallel to the plane of symmetry

c' local chord perpendicular to the wing sweep axis

$\bar{c}$ mean aerodynamic chord, $\frac{\int_0^{b/2} c^2 dy}{\int_0^{b/2} c\, dy}$

c_{l_i} section design lift coefficient

i_t incidence of the horizontal tail with respect to the wing root chord

$\frac{L}{D}$ lift-drag ratio

l_t tail length, longitudinal distance between the quarter points of the mean aerodynamic chords of the wing and the horizontal tail

M free-stream Mach number

q free-stream dynamic pressure

R Reynolds number based on the wing mean aerodynamic chord

S area of semispan wing

S_t area of semispan horizontal tail

t maximum thickness of section

$\bar{V}_t$ horizontal-tail volume, $\frac{S_t l_t}{S\bar{c}}$

y lateral distance from the plane of symmetry

α angle of attack, measured with respect to a reference plane through the leading edge and root chord of the wing

α_t angle of attack of the isolated horizontal tail

ϵ effective average downwash angle

λ taper ratio, ratio of wing tip chord to the wing root chord

φ angle of twist, the angle between the local wing chord and the reference plane through the leading edge and the root chord of the wing (positive for washin and measured in planes parallel to the plane of symmetry)

η fraction of wing semispan, $\frac{y}{b/2}$

$\eta_t\left(\frac{q_t}{q}\right)$ tail efficiency factor (ratio of the lift-curve slope of the horizontal tail when mounted on the fuselage in the flow field of the wing to the lift-curve slope of the isolated horizontal tail)

Subscripts

f fuselage

t horizontal tail

w wing

MODEL

The wing-fuselage and wing-fuselage-tail combinations (fig. 1(a)) employed the twisted and cambered, variable-sweepback wing of reference 1 which had NACA 64A thickness distribution. This distribution of thickness was combined with an $a = 0.8$ modified mean line having an ideal lift coefficient of 0.4 to form the sections perpendicular to the quarter-chord line of the unswept wing panel. The thickness-chord ratios of these sections varied from 14 percent at the root to 11 percent at the tip.

The wing was constructed of solid steel and the surfaces were polished smooth. For this investigation, the angle of sweepback of the wing was 40° and the aspect ratio was 7.0. Twist was introduced by rotating the streamwise sections of the wing at 40° of sweepback about the leading edge while maintaining the projected plan form. The variations of twist and thickness ratio along the semispan are shown in figure 1(b).

The fuselage employed for these tests consisted of a cylindrical midsection with simple fairings fore and aft. Coordinates of the fuselage are listed in table I. The fuselage had a fineness ratio of 12.6 and was

located, with respect to the wing, so that the upper surface of the wing was nearly tangent to the top of the fuselage at the plane of symmetry. The angle of incidence of the wing root with respect to the fuselage center line was 3°. The fuselage was constructed of aluminum bolted to a heavy steel structural member.

The model was tested with several combinations of streamwise fences on the upper surface of the wing. The fences were varied in spanwise position, number, and chordwise extent. The forward portions of the fences which extended from the lower surface around the leading edge of the wing to 0.10 chord and the rear portion of the fences which extended from 0.75 chord to the trailing edge of the wing could be removed to effect the changes in the chordwise extent of the fences. Details of the fences are shown in figure 2.

The all-movable horizontal tail had an aspect ratio of 3.0, a taper ratio of 0.5, and 40° of sweepback. The axis about which the incidence of the horizontal tail was varied was at 53.4 percent of the tail root chord. This hinge axis was at the intersection of the fuselage center line and the plane of the wing root chord (see fig. 1(a)). Tail volume was 0.497. The tail was constructed of solid steel and the surfaces were polished smooth.

Figure 3 is a photograph of the model mounted in the wind tunnel. The turntable upon which the model was mounted is directly connected to the balance system.

CORRECTIONS TO DATA

The data have been corrected for constriction effects due to the presence of the tunnel walls by the method of reference 3, for tunnel-wall interference originating from lift on the model by the method of reference 4, and for drag tares caused by aerodynamic forces on the turntable upon which the model was mounted.

The corrections to dynamic pressure, Mach number, angle of attack, drag coefficient, and to pitching-moment coefficient were the same as those used for reference 2 and are listed in table II.

RESULTS AND DISCUSSION

Tests were conducted to determine the best fence arrangement, the longitudinal characteristics of the wing-fuselage combination with the best fences, and the longitudinal characteristics of the wing-fuselage-tail combination with the best fences. The results of these tests are shown in figures 4 through 7, 8 through 15, and 16 through 24, respectively.

Wing-Fuselage Combination

Selection of fences.- The tests to determine the most satisfactory fences were conducted with the tail off. The design and location of the fences were based on the flow studies shown in reference 1 and the results of the fence investigation reported in reference 2.

Figures 4 through 7 show, for a Mach number of 0.417, the effects of varying the number of fences, the spanwise location of the fences, and the chordwise extent of the fences on the longitudinal characteristics. The addition of fences had only small effect on the lift coefficient at which large changes in longitudinal stability occurred; however, the fences decreased the severity of these changes. The largest improvement in stability was obtained with full-chord fences at 33, 50, 70, and 85 percent of the semispan. Fences extending from 0.10 chord to the trailing edge at the same semispan locations provided almost the same improvements in stability with slightly less drag at the lower lift coefficients (fig. 7). These fences are referred to hereinafter as the partial-chord fences.

The wing-fuselage combination was tested with and without the complete- and partial-chord fences at 33, 50, 70, and 85 percent of the semispan at a Mach number of 0.25 and a Reynolds number of 8 million and at Mach numbers from 0.25 to 0.92 at a Reynolds number of 2 million. The results of these tests are shown in figures 8 through 11. The addition of fences usually increased the lift-curve slopes and reduced the drag at the higher lift coefficients; however, at the lower lift coefficients, the fences increased the drag moderately. These effects of fences on drag are best shown in figure 12 which compares the lift-drag ratios of the wing-fuselage combination with and without fences at several Mach numbers. The effects of the fences on the pitching-moment characteristics of the wing-fuselage combination were large. At a Mach number of 0.25 and a Reynolds number of 8 million, the lift coefficient at which large changes in stability occurred was increased by the fences to values as great as 1.15. At a Reynolds number of 2 million and at Mach numbers less than 0.83, the addition of fences did not increase the lift coefficient at which large changes in stability occurred; however, the fences greatly reduced the magnitude of these changes. At higher Mach numbers, the fences were very effective in delaying changes in stability to higher lift coefficients. This effect of fences increased with Mach number at supercritical speeds.

Effects of Mach number.- The effects of Mach number on the lift and pitching-moment-curve slopes at a lift coefficient of 0.40 and on the drag characteristics are shown in figures 13 and 14. The lift and stability characteristics (fig. 13) of the combination with fences were less affected by increasing Mach number than those of the combination without fences. In particular, the large decreases in lift-curve slope and stability indicated for the combination at supercritical speeds were eliminated or delayed by the addition of fences.

The Mach numbers for drag divergence of the combination (defined as $dC_D/dM = 0.10$) were slightly higher for the combination with fences than for the combination without fences (fig. 14); however, the drag coefficients of the combinations with fences were usually higher than those corresponding to the divergence Mach numbers of the combination without fences. These values are presented for both the full- and partial-chord fences in the following table:

C_L	M for drag divergence			$C_{D_{divergence}}$		
	Fences off	Full-chord fences	Partial-chord fences	Fences off	Full-chord fences	Partial-chord fences
0.20	0.905	0.900	0.900	0.0190	0.0210	0.0200
.40	.840	.860	.855	.0235	.0265	.0250
.50	.820	.835	.835	.0265	.0305	.0295
.60	.815	.820	.820	.0330	.0380	.0365

Effects of Reynolds number.- The effect of increasing Reynolds number from 2 million to 8 million on the longitudinal characteristics of the wing-fuselage combination was large at a Mach number of 0.25. This increase in Reynolds number about doubled the lift coefficient at which large changes in stability first appeared for the model without fences (figs. 8 and 10). At a Reynolds number of 2 million, the fences were ineffectual in delaying large changes in stability to higher lift coefficients, but at a Reynolds number of 8 million, the fences increased this lift coefficient from about 0.80 to values in excess of 1.0. The lift-drag ratios (see fig. 12) of the combination at high lift coefficients were considerably lower at a Reynolds number of 2 million than at a Reynolds number of 8 million.

It is possible that the test results at Mach numbers greater than 0.25 may have been affected by the comparatively low Reynolds number (2 million) at which they were obtained. Caution should be exercised in applying these results to the prediction of the characteristics of a full-scale airplane.

Effects of section.- Figure 15 compares the longitudinal characteristics of the wing-fuselage combination of reference 2 (four-digit thickness distribution) with those of the subject model. The combinations were identical except for wing thickness distribution. The comparisons are shown for the combinations with and without partial-chord fences (0.10c to the trailing edge) at 33, 50, 70, and 85 percent of the semispan. At a lift coefficient of 0.40 and at Mach numbers greater than about 0.55, the 64A combination with fences had greater stability than the four-digit combination with fences. Also, at a lift coefficient of 0.40, the 64A combination with fences had less drag at subcritical speeds than the four-digit combination with fences, but at supercritical speeds the four-digit combination with fences had the least drag. The Mach numbers and drag

coefficients for drag divergence for both combinations with and without fences are shown for a lift coefficient of 0.40 in the following table:

Wing	M for drag divergence		$C_{D_{divergence}}$	
	Fences off	Fences on	Fences off	Fences on
64A	0.840	0.855	0.0235	0.0250
Four-digit	.860	.866	.0235	.0258

Wing-Fuselage-Tail Combination

Effects of wing fences.- The wing-fuselage-tail combination was tested with and without the best arrangement of full-chord fences. The results are presented in figures 16 and 17 and are summarized in figures 18 through 21. For the conditions of low speed and high Reynolds number and of high speeds and moderate lift coefficients, the fences did not significantly affect the tail contribution to stability (fig. 18); but, as was the case with the wing-body combination, did increase the lift coefficients at which large changes in longitudinal stability first occurred. The fences did not prevent sizable decreases in longitudinal stability at Mach numbers of 0.60 and 0.70; however, it is thought that this might be an effect of the low Reynolds number (2 million) at which these data were obtained. Figure 19 compares the variation of inflection lift coefficient with Mach number for the subject wing-fuselage-tail combination (64A thickness distribution) and the wing-fuselage-tail combination of reference 2 which employed a wing with four-digit thickness distribution. (As used herein, inflection lift coefficient is arbitrarily defined as the lowest positive lift coefficient at which $(dC_m/dC_L) = 0$.) The four-digit combination apparently had the higher inflection lift coefficients at Mach numbers below 0.86, but the 64A combination had the higher inflection lift coefficients at Mach numbers greater than 0.86.

Effects of Mach number.- Figures 20 and 21 show the variations with Mach number of the slopes of the lift and pitching-moment curves and the drag coefficients of the wing-fuselage-tail combination. The effects of Mach number on these parameters were generally similar to those indicated for the tail-off configuration. The slopes of the lift and pitching-moment curves of the combination with fences appeared to be less affected by increasing Mach number than the slopes of the combination without fences, and the fences did not significantly affect the Mach numbers for drag divergence.

Longitudinal characteristics of the wing-fuselage-tail combination.- The combination was tested with a horizontal tail at two angles of incidence to determine the effect of the tail on the longitudinal

characteristics and the effectiveness of the tail as a longitudinal control. The results of these tests without and with wing fences are shown by the lift, drag, and pitching-moment data in figures 16 and 17. These data show that at most Mach numbers the addition of the tail had only small effect on the lift and drag of the combination with or without fences. The lift coefficients at which large changes in longitudinal stability first occurred were usually higher with the tail than without it.

The factors which determine the tail contribution to the stability are shown in figure 22 as a function of angle of attack for several test conditions. The method used to calculate the effective downwash angle ϵ, the tail efficiency factor $\eta_t(q_t/q)$, and the ratio of the lift-curve slope for the isolated tail to the lift-curve slope of the wing-fuselage combination a_t/a_{w+t} was the same as that used in reference 2. The results of these calculations show that the higher inflection lift coefficients attained with the tail on were mostly due to an increase in the factor a_t/a_{w+t} with increasing lift coefficient in a manner which offset the reduction in stability of the wing-fuselage combination at high lift. This was true at most Mach numbers. At the higher lift coefficients, the rate of change of downwash with angle of attack and the tail efficiency factors were usually higher for the combination without fences than for the combination with fences. Figure 23 shows the variation with Mach number of the tail-control effectiveness parameter $\partial C_m/\partial i_t$. This parameter generally increased moderately with increasing Mach number and was slightly larger for the combination without fences than for the combination with fences. Figure 24 shows that the variations with Mach number of the factors affecting the stability contribution of the horizontal tail were small.

CONCLUSIONS

A wind-tunnel investigation has been made of a wing-fuselage and a wing-fuselage-tail combination having a wing sweptback 40° with an aspect ratio of 7.0 and NACA 64A thickness distribution. The following conclusions were indicated:

1. The addition of multiple wing fences to the wing-fuselage and wing-fuselage-tail combinations eliminated large changes in longitudinal stability up to lift coefficients in excess of 1.0 at a Mach number of 0.25 and a Reynolds number of 8 million, an improvement of as much as 50 percent over the values with the fences off. At high subcritical and supercritical speeds, large changes in stability occurred at lift coefficients near 0.60 for the wing-fuselage-tail combination without fences. Fences delayed these changes to lift coefficients between 0.70 and 0.80.

2. Adding fences to the wings increased the drag of the wing-fuselage combination moderately at low lift coefficients, but usually reduced the drag and increased the lift-drag ratios at the higher lift coefficients.

3. The Mach numbers for drag divergence of the combination were increased slightly by the addition of fences; however, the corresponding drag coefficients were higher than those corresponding to the divergence Mach numbers of the combination without fences.

4. The fences had little effect on the tail contribution to stability at low speed and high Reynolds number and at moderate lift coefficients at high speeds.

5. The all-movable horizontal tail had nearly constant control effectiveness throughout the lift range at most Mach numbers and its effectiveness as a longitudinal control at an angle of attack of 4° was usually increased moderately by increasing Mach number.

Ames Aeronautical Laboratory
National Advisory Committee for Aeronautics
Moffett Field, Calif., Mar. 30, 1955

REFERENCES

1. Sutton, Fred B., and Dickson, Jerald K.: A Comparison of the Longitudinal Aerodynamic Characteristics at Mach Numbers Up to 0.94 of Sweptback Wings Having NACA 4-Digit or NACA 64A Thickness Distributions. NACA RM A54F18, 1954.

2. Sutton, Fred B., and Dickson, Jerald K.: The Longitudinal Characteristics at Mach Numbers Up to 0.92 of Several Wing-Fuselage-Tail Combinations Having Sweptback Wings With NACA Four-Digit Thickness Distributions. NACA RM A54L08, 1955.

3. Herriot, John G.: Blockage Corrections for Three-Dimensional-Flow Closed-Throat Wind Tunnels, With Consideration of the Effect of Compressibility. NACA Rep. 995, 1950. (Formerly NACA RM A7B28.)

4. Sivells, James C., and Salmi, Rachel M.: Jet-Boundary Corrections for Complete and Semispan Swept Wings in Closed Circular Wind Tunnels. NACA TN 2454, 1951.

TABLE I.- FUSELAGE COORDINATES

Distance from nose, in.	Radius, in.
0	0
1.27	1.04
2.54	1.57
5.08	2.35
10.16	3.36
20.31	4.44
30.47	4.90
39.44	5.00
50.00	5.00
60.00	5.00
70.00	5.00
76.00	4.96
82.00	4.83
88.00	4.61
94.00	4.27
100.00	3.77
106.00	3.03
126.00	0

TABLE II.- CORRECTIONS TO DATA

(a) Corrections for constriction effects

Corrected Mach number	Uncorrected Mach number	$\frac{q_{corrected}}{q_{uncorrected}}$
0.25	0.250	1.003
.60	.599	1.006
.70	.696	1.007
.80	.793	1.010
.83	.821	1.012
.86	.848	1.015
.88	.866	1.017
.90	.883	1.020
.92	.899	1.024

(b) Corrections for tunnel-wall interference

$\Delta\alpha = 0.455C_L$

$\Delta C_D = 0.00662C_L^2$

$\Delta C_{m_{tail\ off}} = K_1 C_{L_{tail\ off}}$

$$\Delta C_{m_{tail\ on}} = K_1 C_{L_{tail\ off}} - \left[(K_2 C_{L_{tail\ off}} - \Delta\alpha)\frac{\partial C_m}{\partial i_t}\right]$$

where:

M	K_1	K_2
0.25	0.0027	0.72
.60	.0038	.74
.70	.0043	.76
.80	.0049	.79
.83	.0050	.80
.86	.0053	.83
.88	.0054	.84
.90	.0056	.86
.92	.0057	.88

Notes:

(1) Wing sections perpendicular to the sweep axis have NACA 64A thickness distributions combined with an NACA $a = 0.8$ (modified) mean line, $c_{l_i} = 0.4$.

(2) Horizontal tail sections perpendicular to the sweep axis have NACA 0010 thickness distributions.

(3) All dimensions in inches and areas in square feet.

$A = 7.00$	$\lambda = 0.4$
$S = 5.92$	$\lambda_t = 0.5$
$S_t = 1.05$	$\bar{V}_t = 0.497$

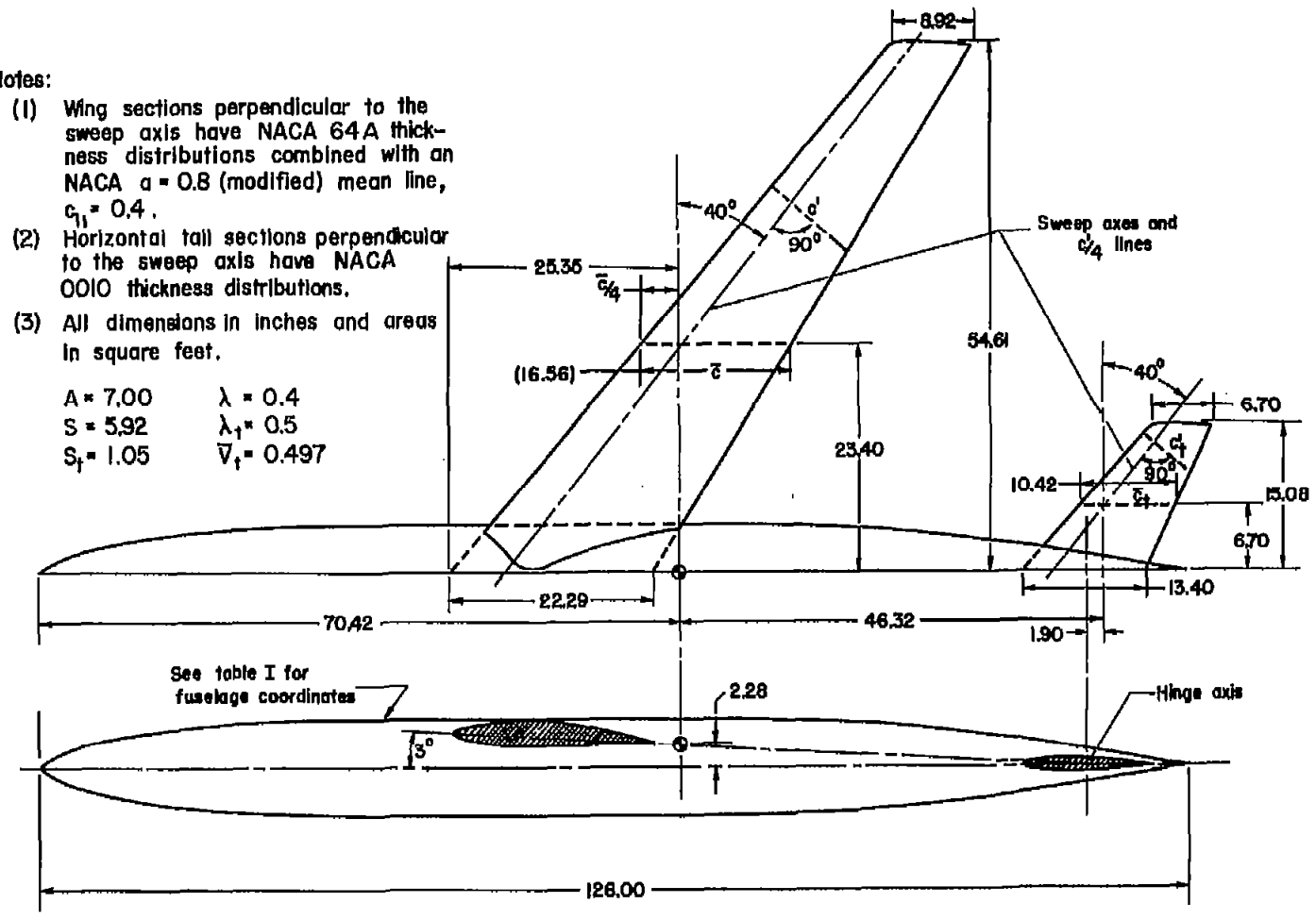

(a) Dimensions

Figure 1.- Geometry of the model.

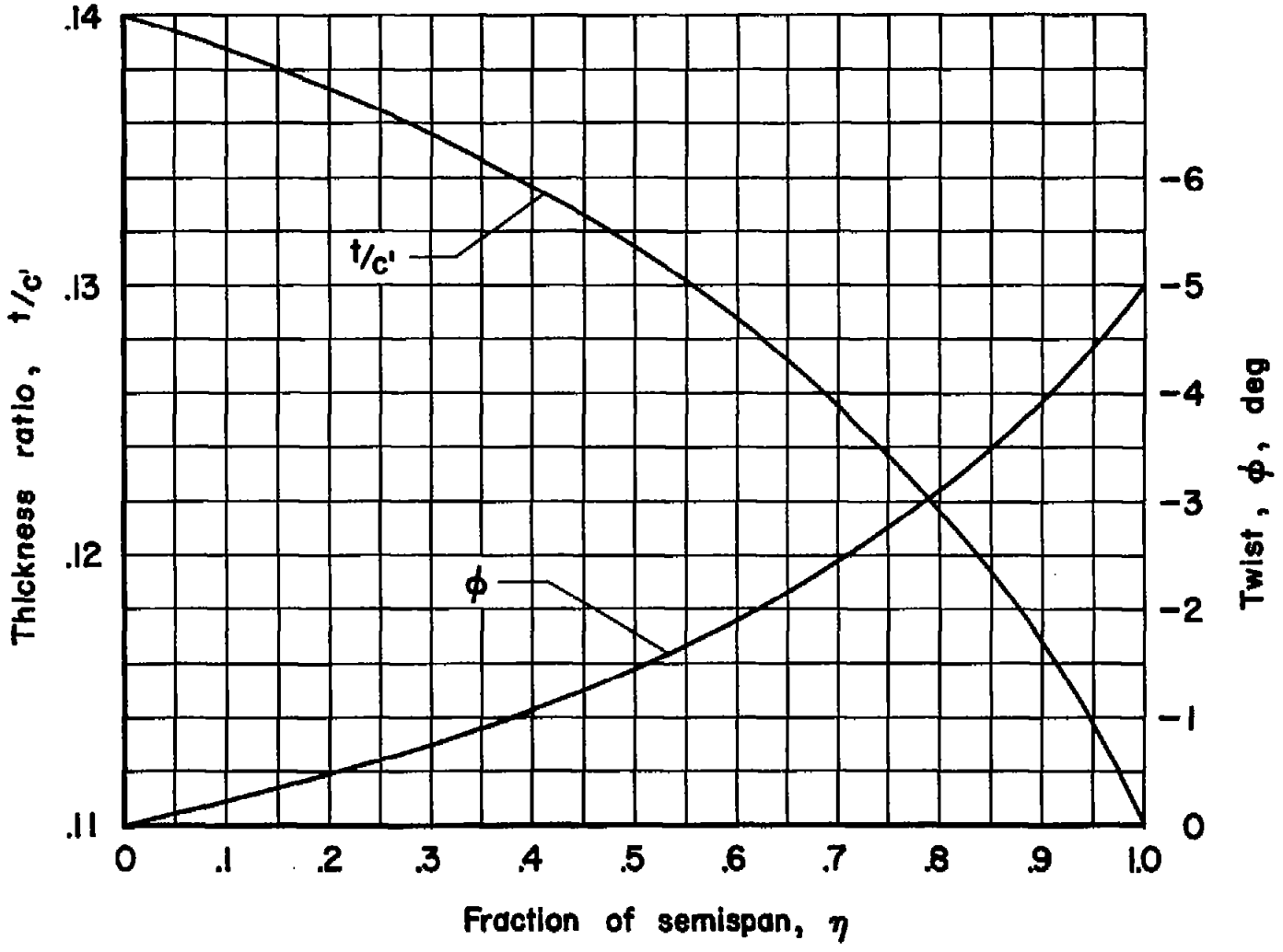

(b) Distribution of twist and thickness ratio.

Figure 1.- Concluded.

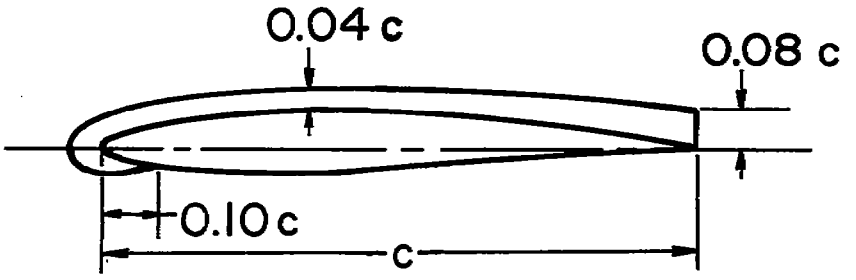

Full-chord fence

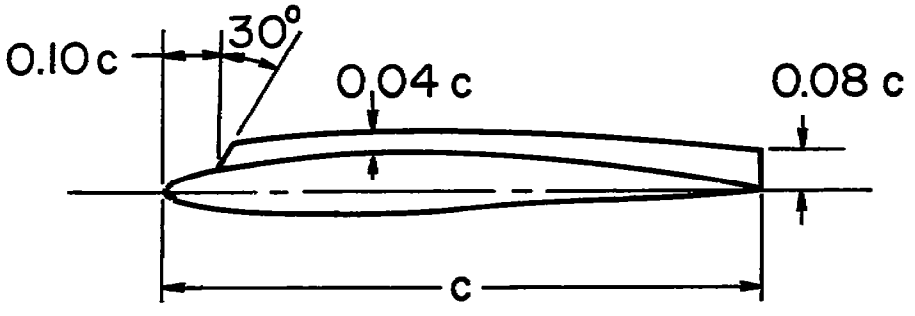

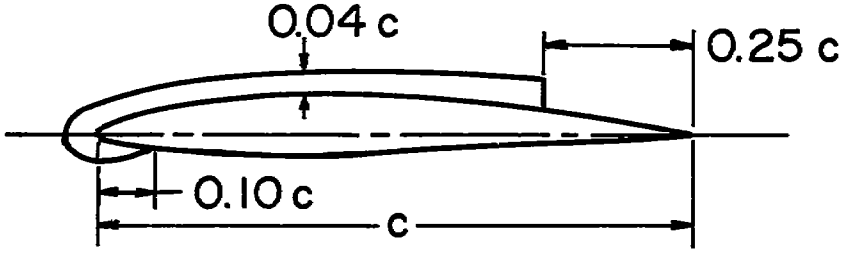

Partial-chord fences

Figure 2.- Fence details.

A-19214

Figure 3.- Photograph of the model.

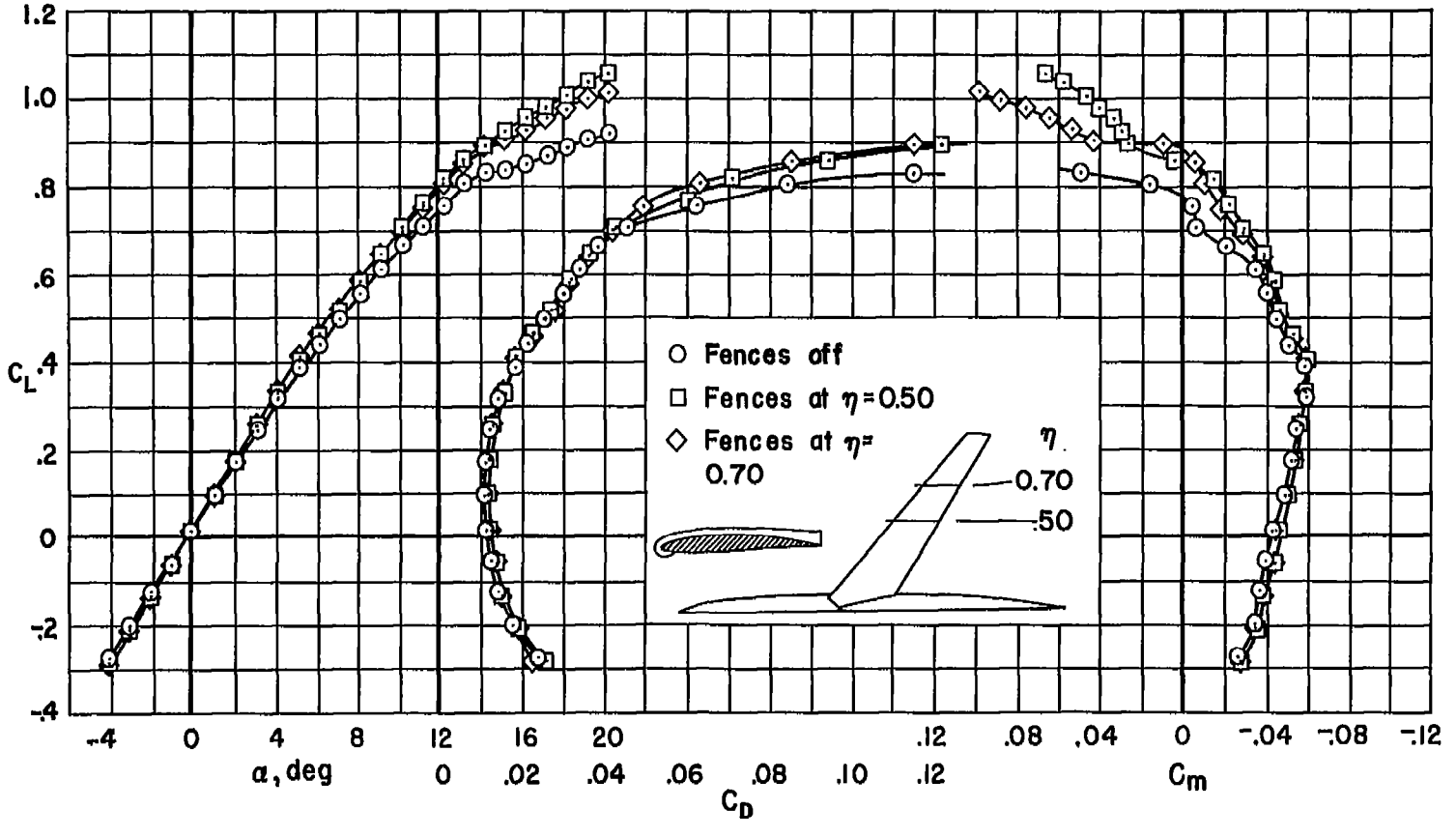

Figure 4.- The effect of a single wing fence at various spanwise locations on the longitudinal characteristics of the wing-fuselage combination; M = 0.417, R = 3,600,000.

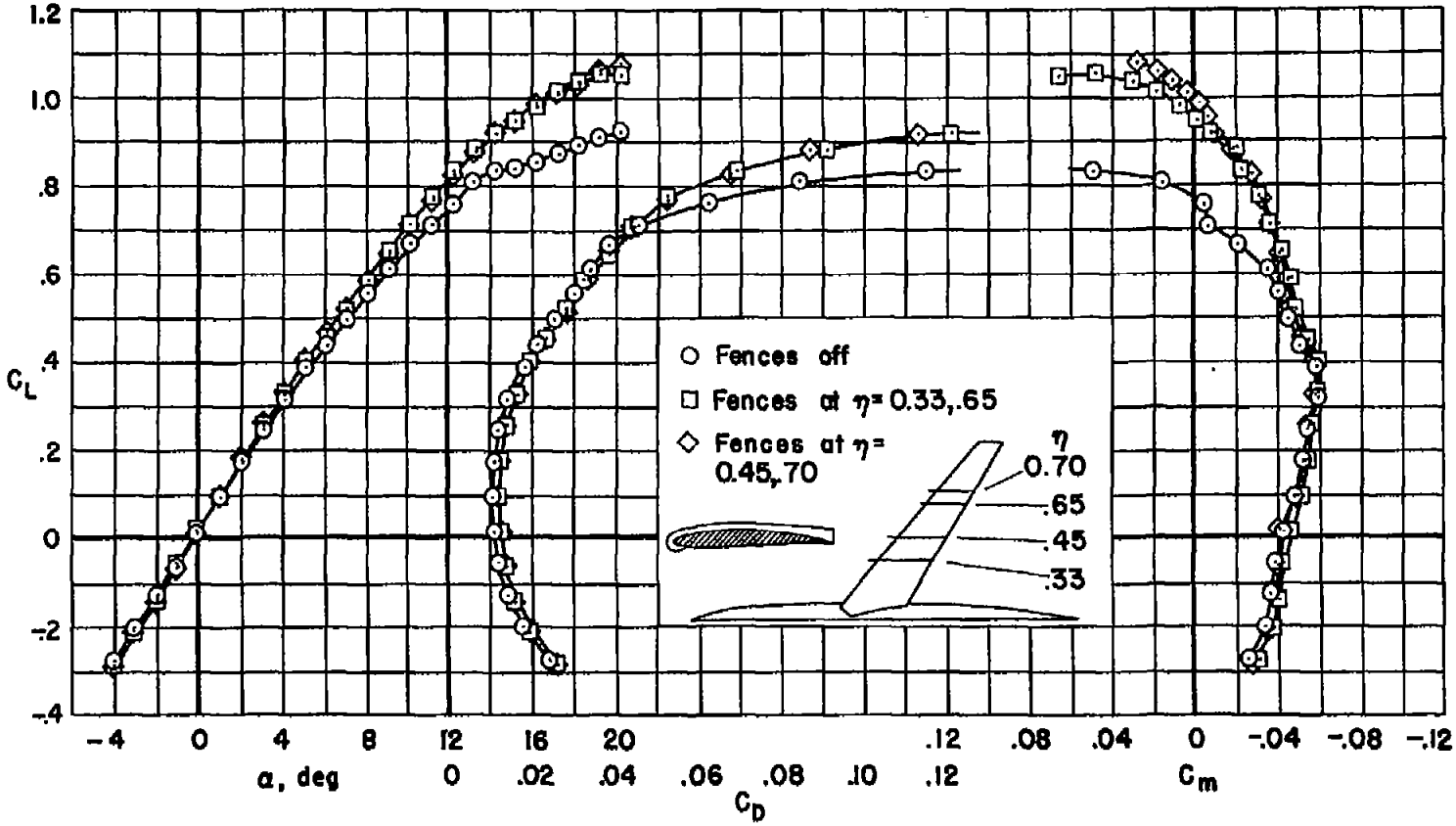

Figure 5.- The effect of two fences at various spanwise locations on the longitudinal characteristics of the wing-fuselage combination; M = 0.417, R = 3,600,000.

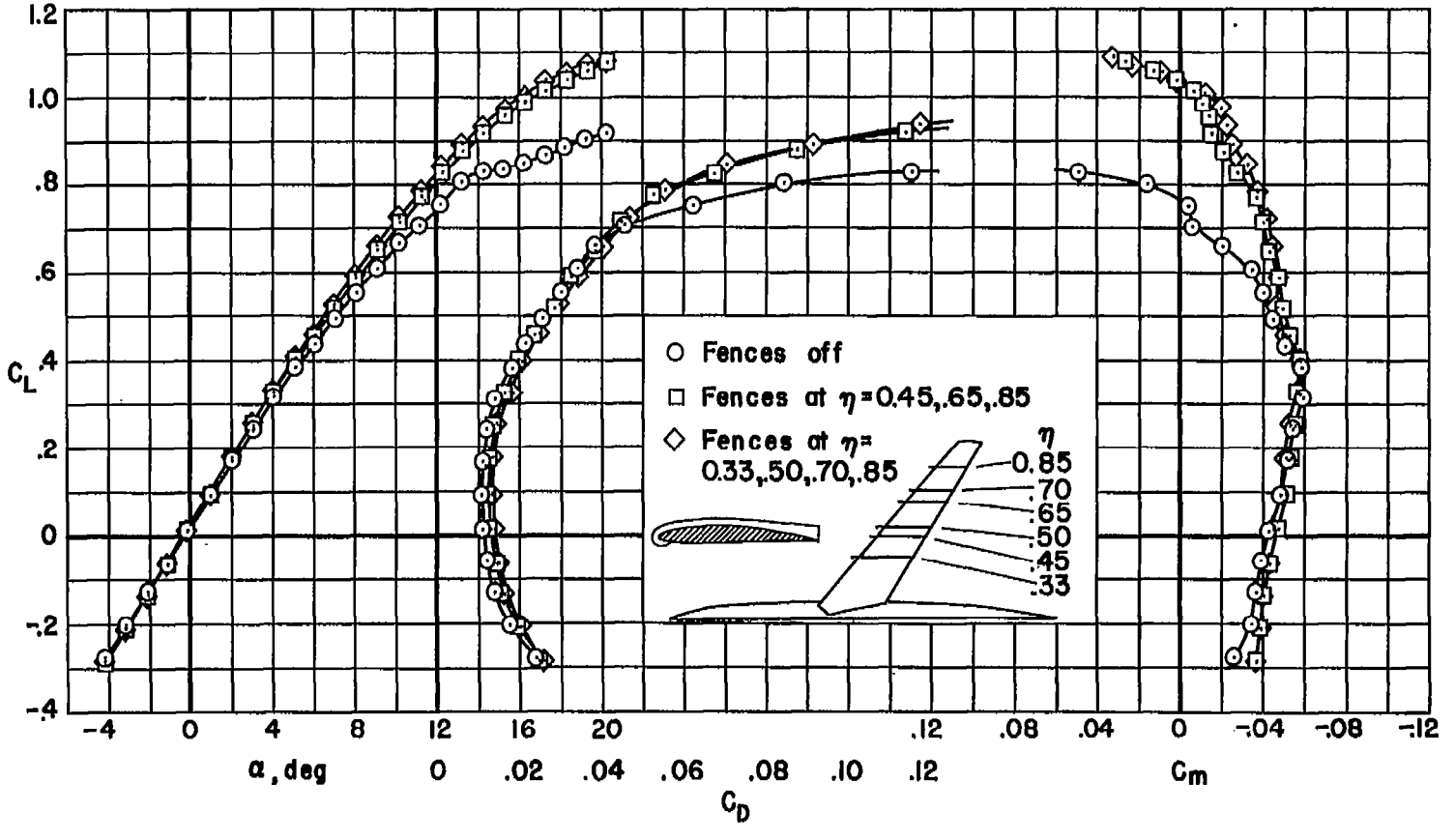

Figure 6.- The effect of three and four fences on the longitudinal characteristics of the wing-fuselage combination; M = 0.417, R = 3,600,000.

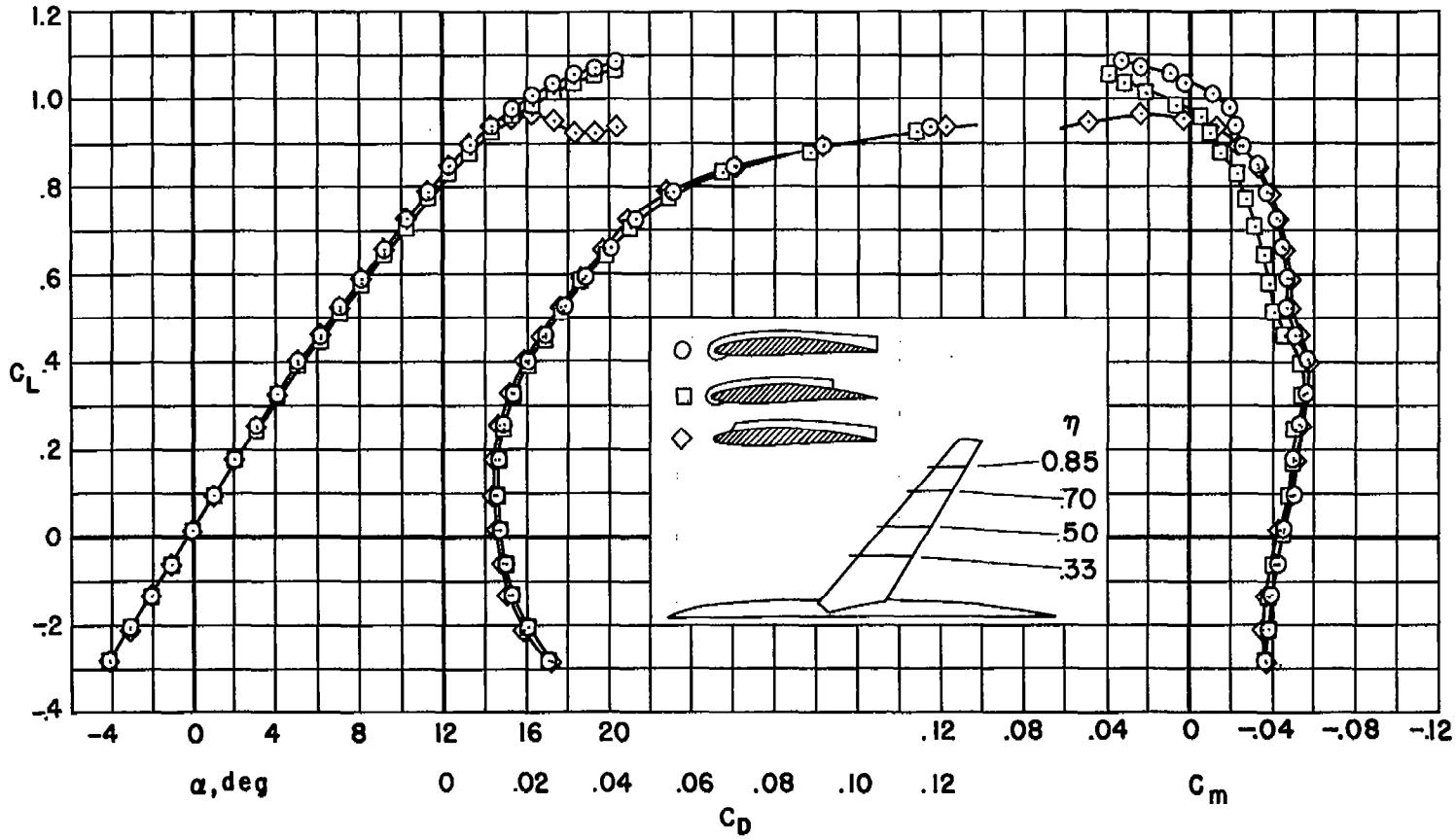

Figure 7.- The effect of complete- and partial-chord fences on the longitudinal characteristics of the wing-fuselage combination; M = 0.417, R = 3,600,000.

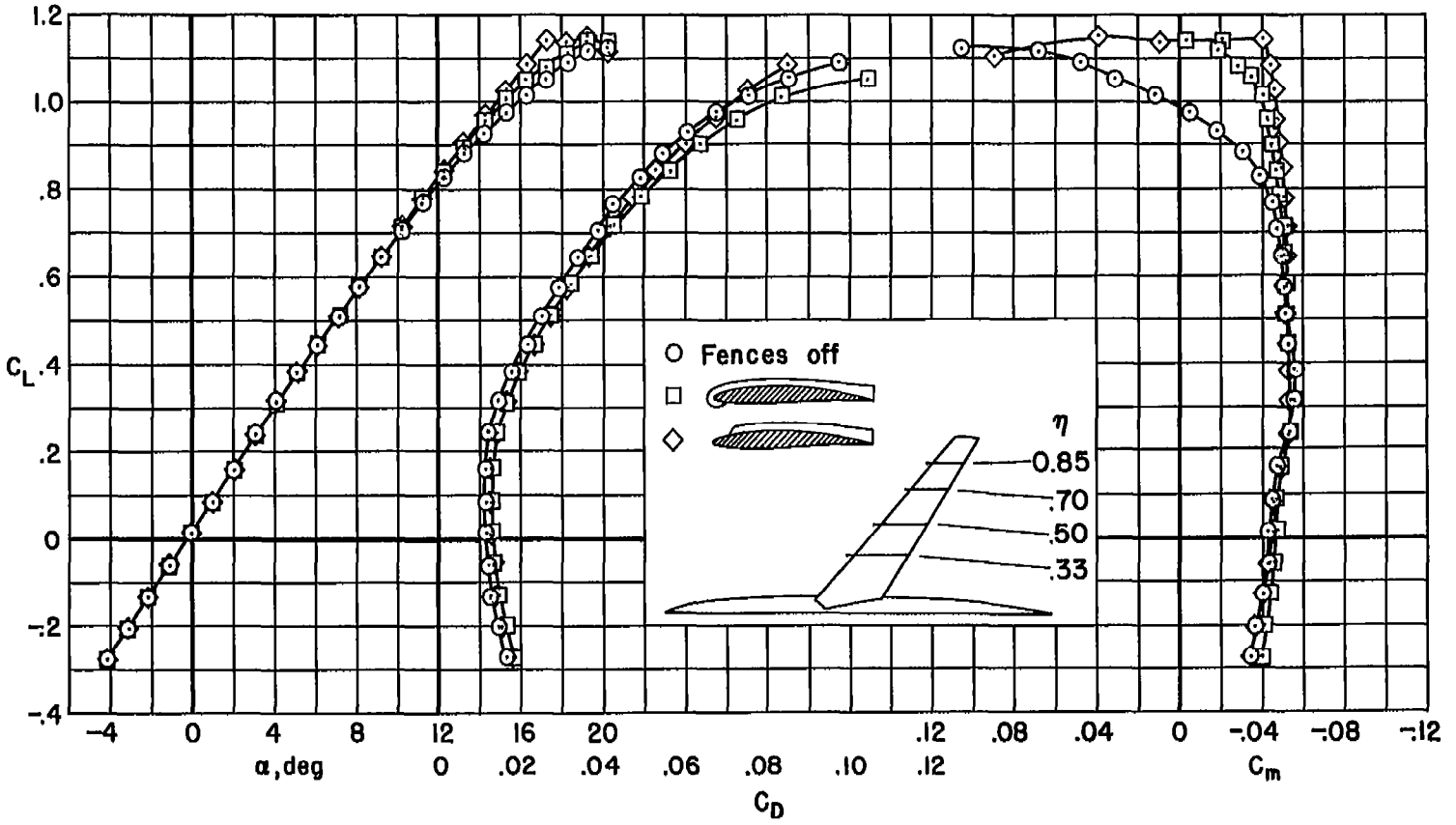

Figure 8.- The effect of complete- and partial-chord fences on the longitudinal characteristics of the wing-fuselage combination; M = 0.25, R = 8×10^6.

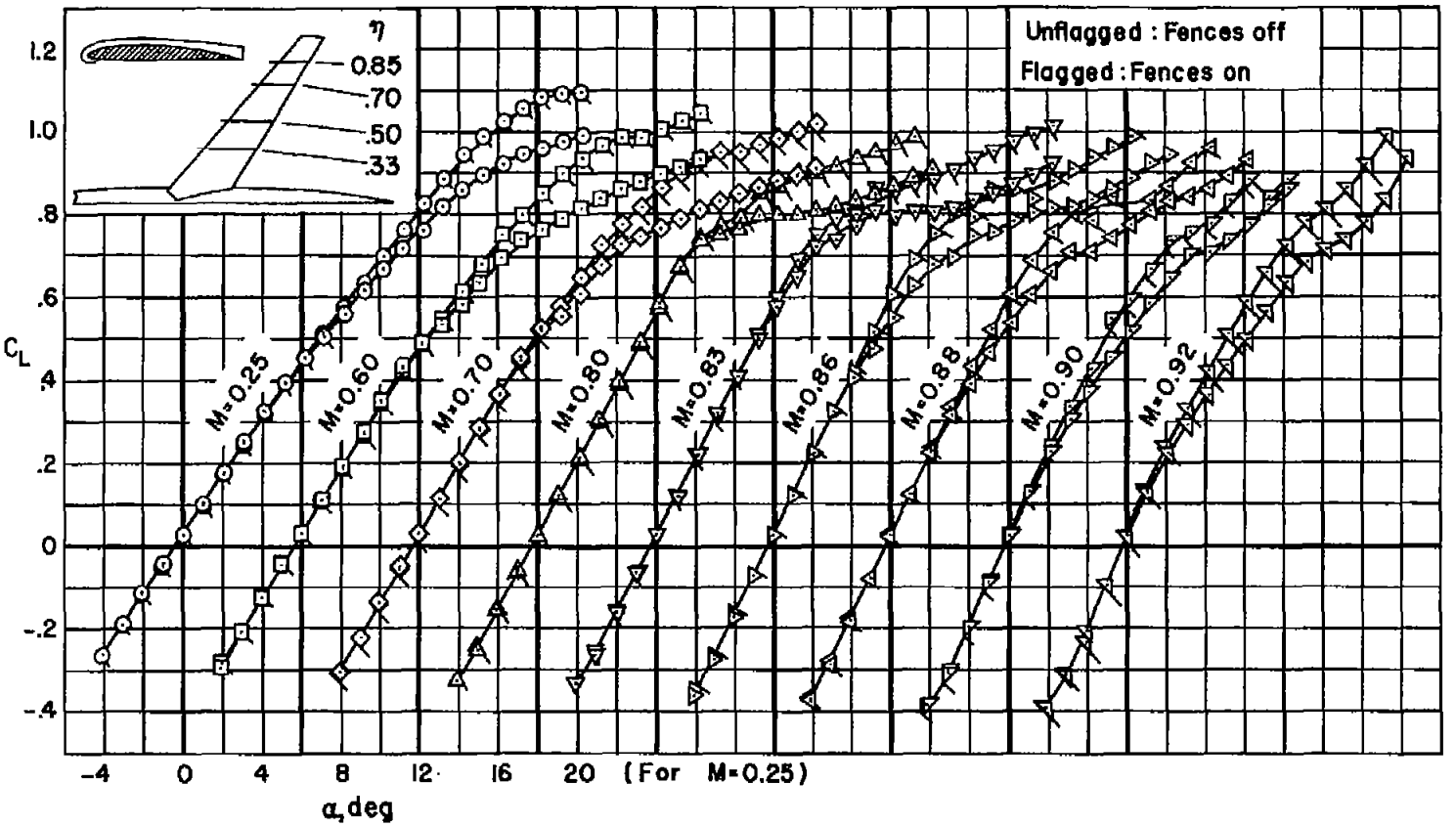

(a) Complete-chord fences.

Figure 9.- The effect of complete- and partial-chord fences on the lift characteristics of the wing-fuselage combination at several Mach numbers; R = 2,000,000.

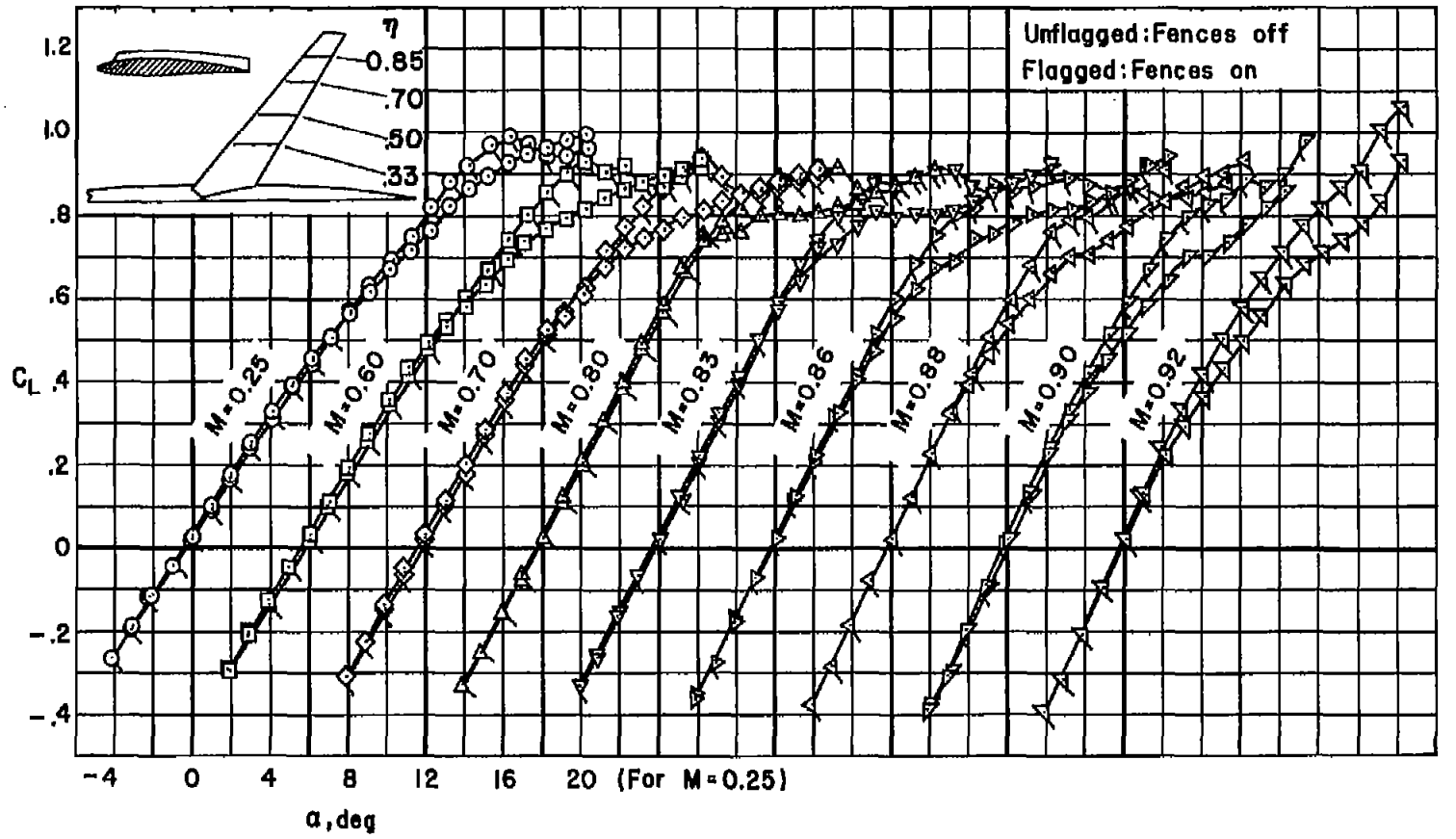

(b) Partial-chord fences.

Figure 9.- Concluded.

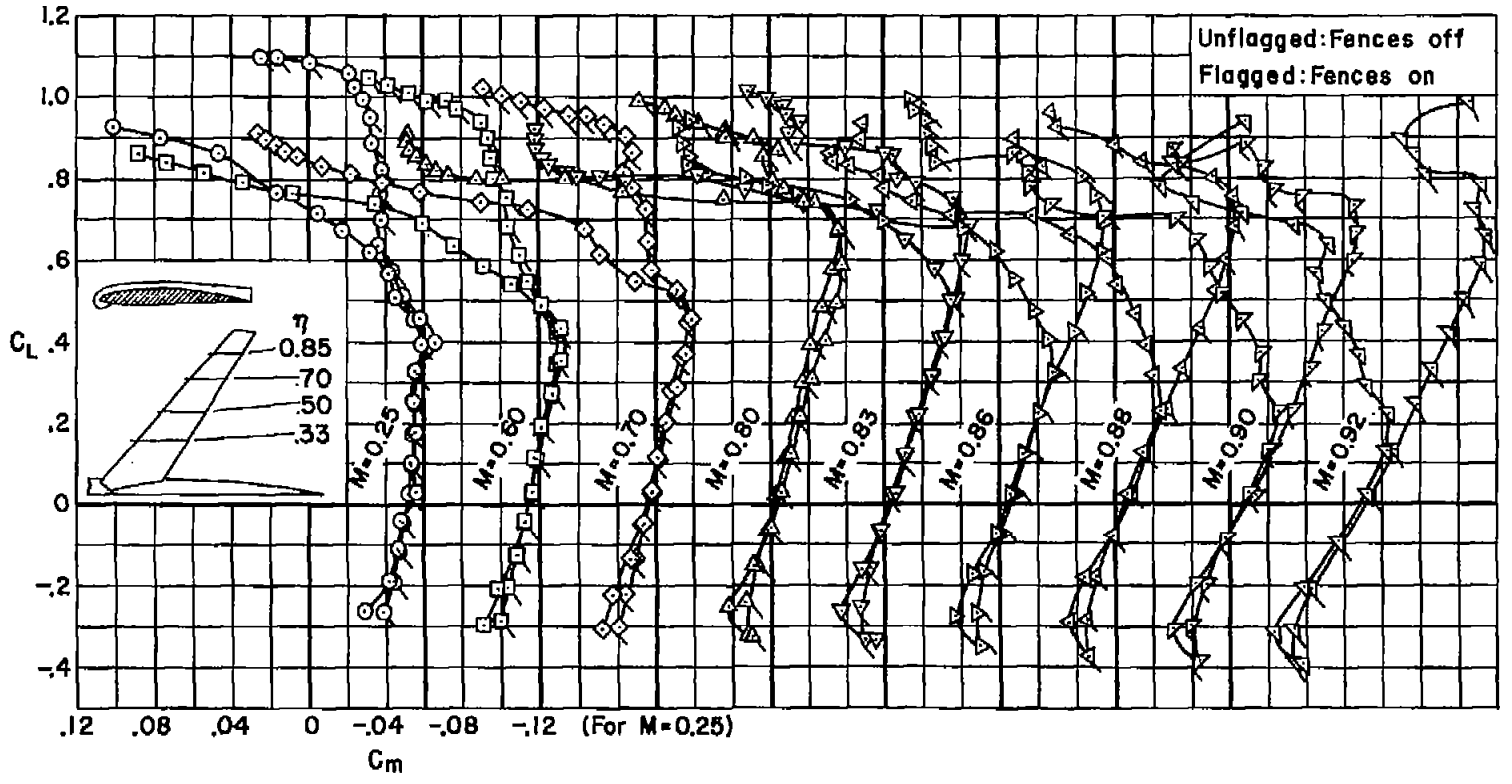

(a) Complete-chord fences.

Figure 10.- The effect of complete- and partial-chord fences on the pitching-moment characteristics of the wing-fuselage combination at several Mach numbers; R = 2,000,000.

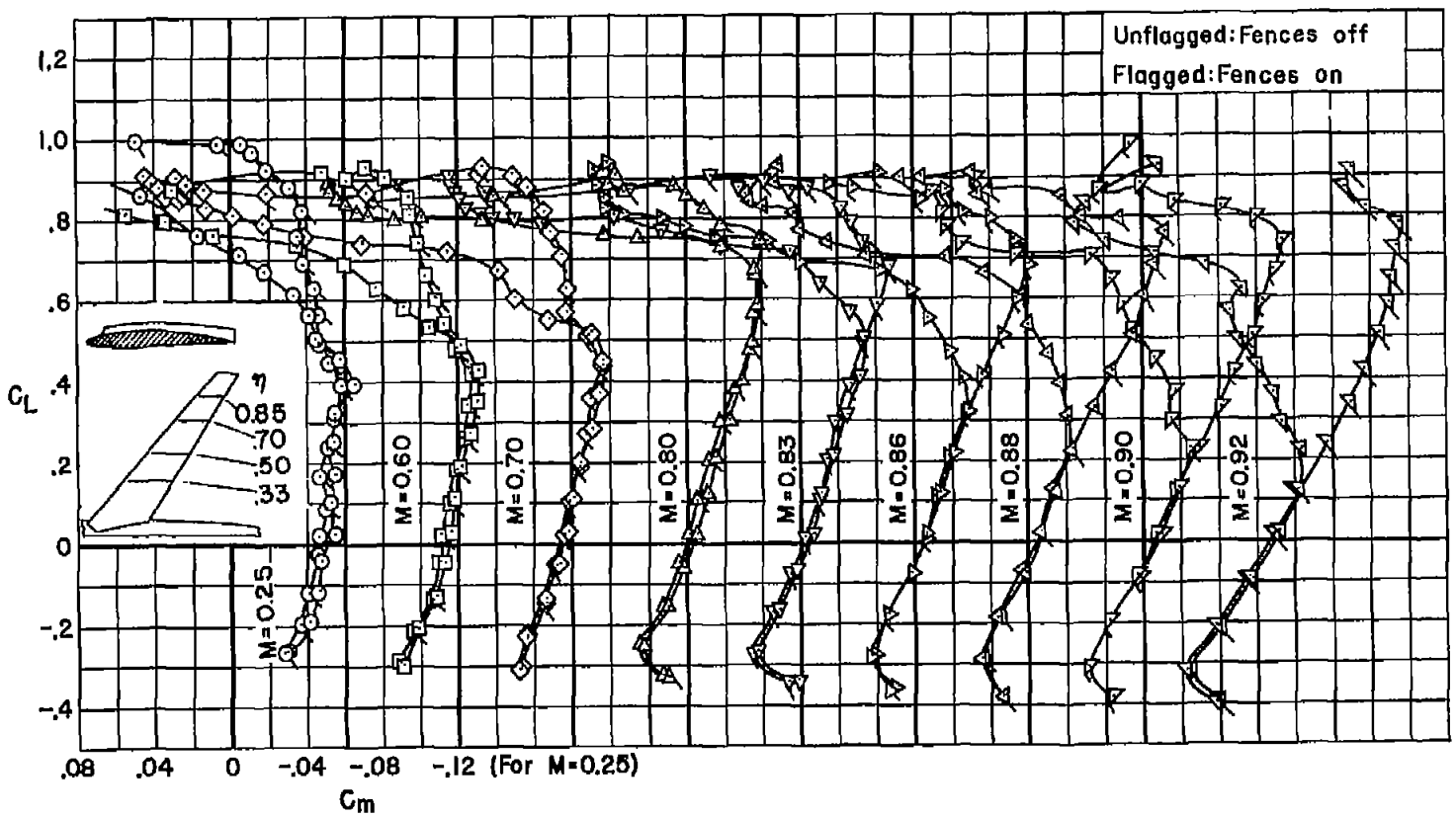

(b) Partial-chord fences.

Figure 10.- Concluded.

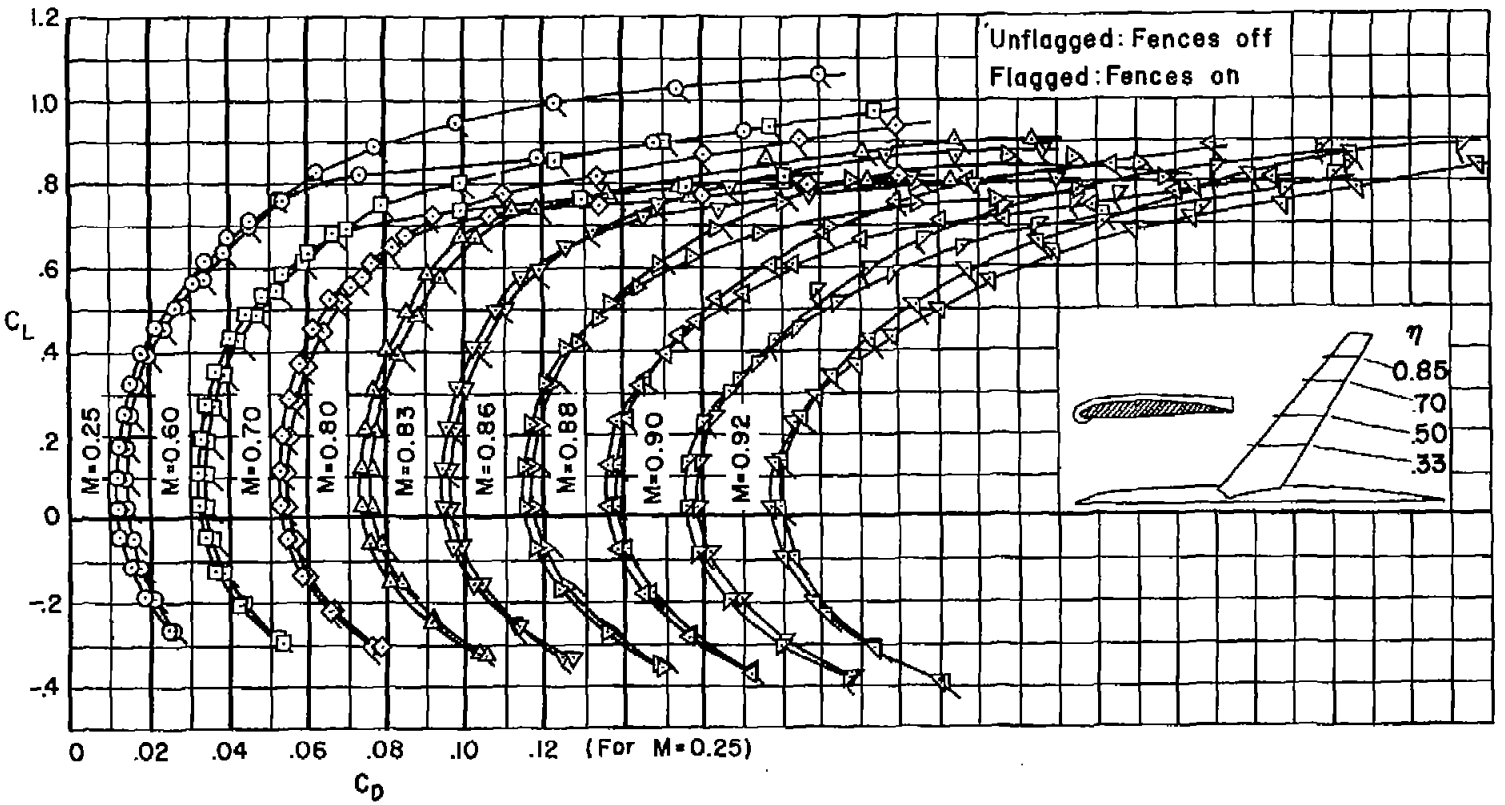

(a) Complete-chord fence.

Figure 11.- The effect of complete- and partial-chord fences on the drag characteristics of the wing-fuselage combination at several Mach numbers; R = 2,000,000.

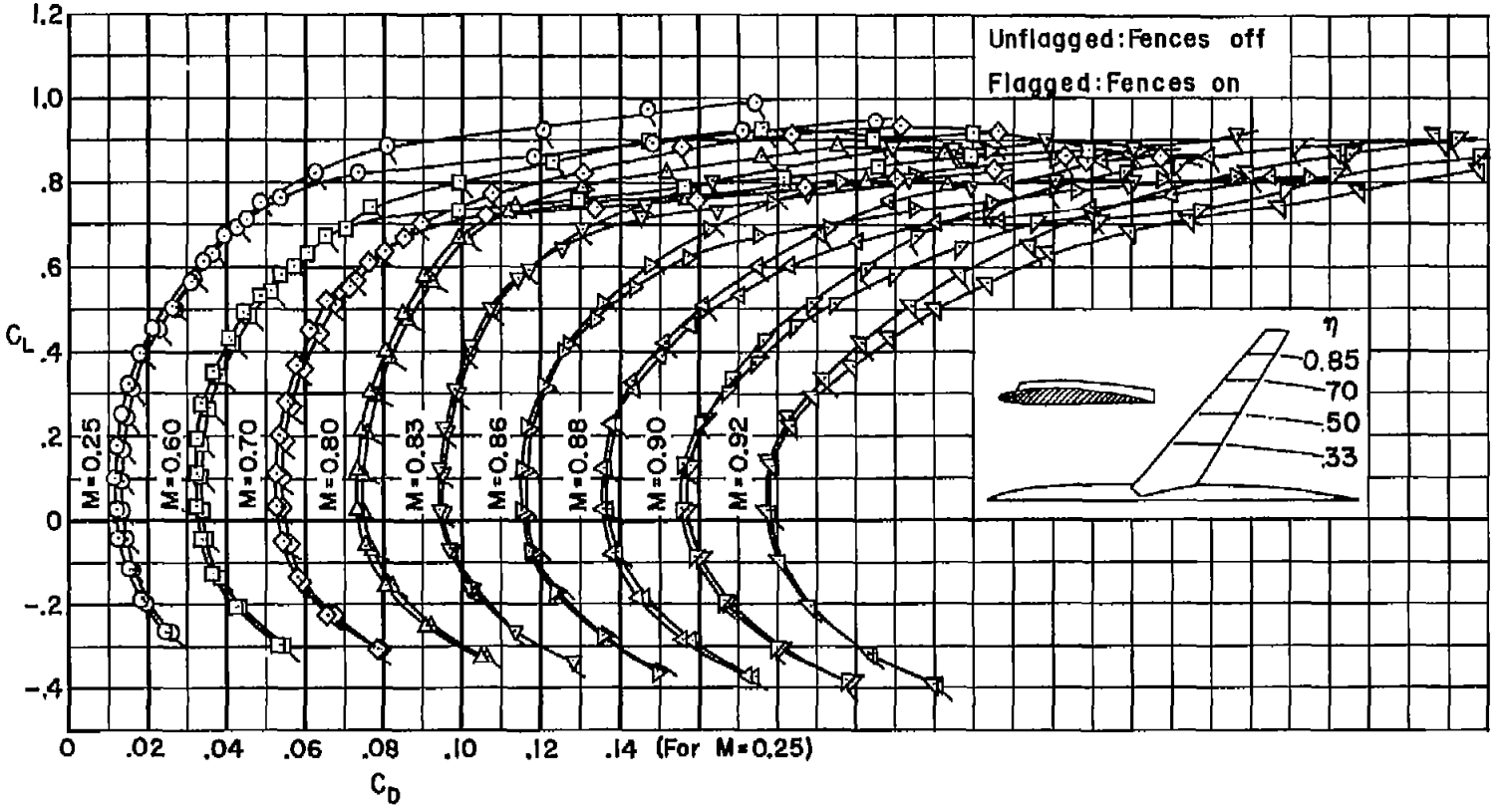

(b) Partial-chord fence.

Figure 11.- Concluded.

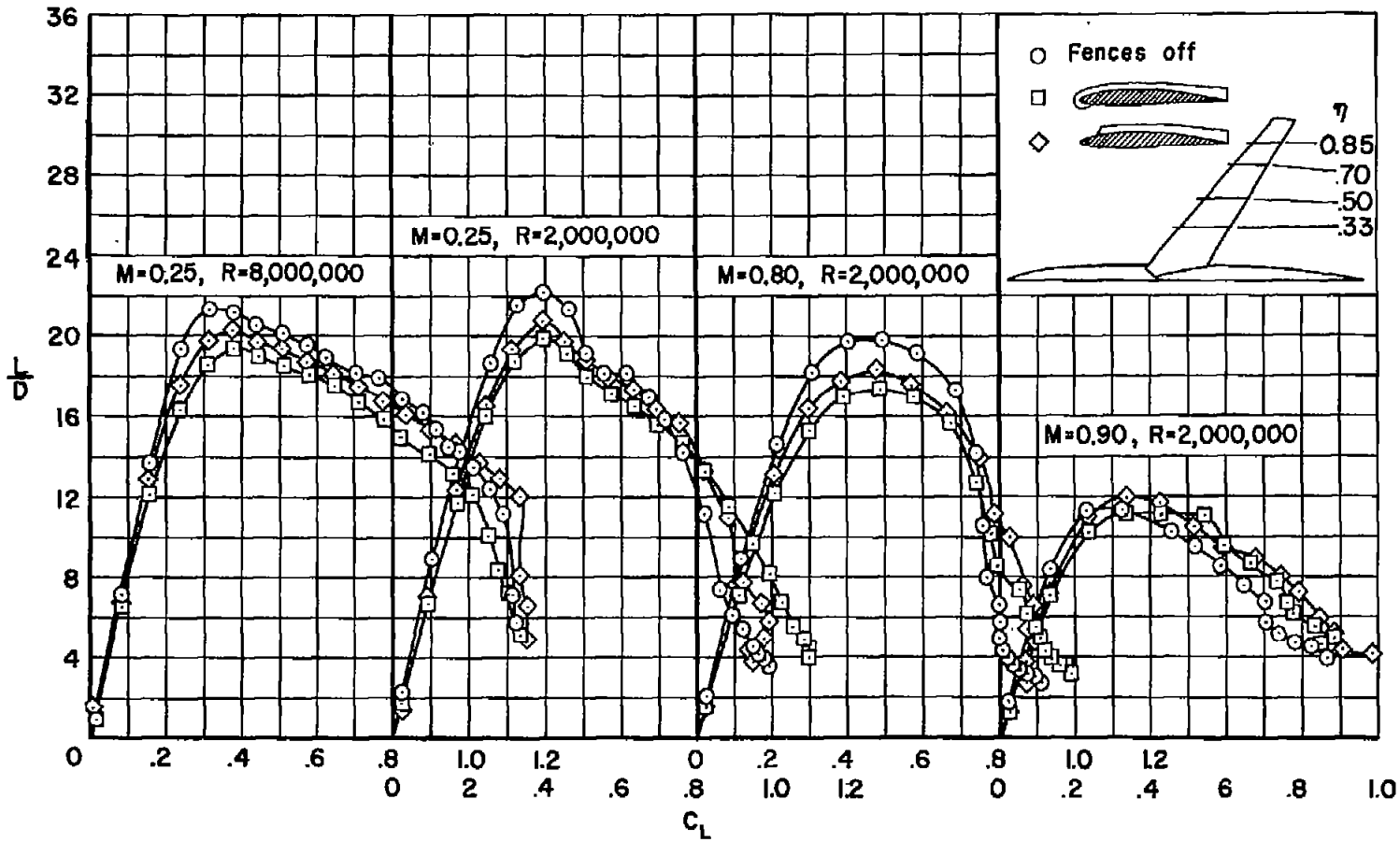

Figure 12.- The effect of complete- and partial-chord fences on the lift-drag ratios of the wing-fuselage combination.

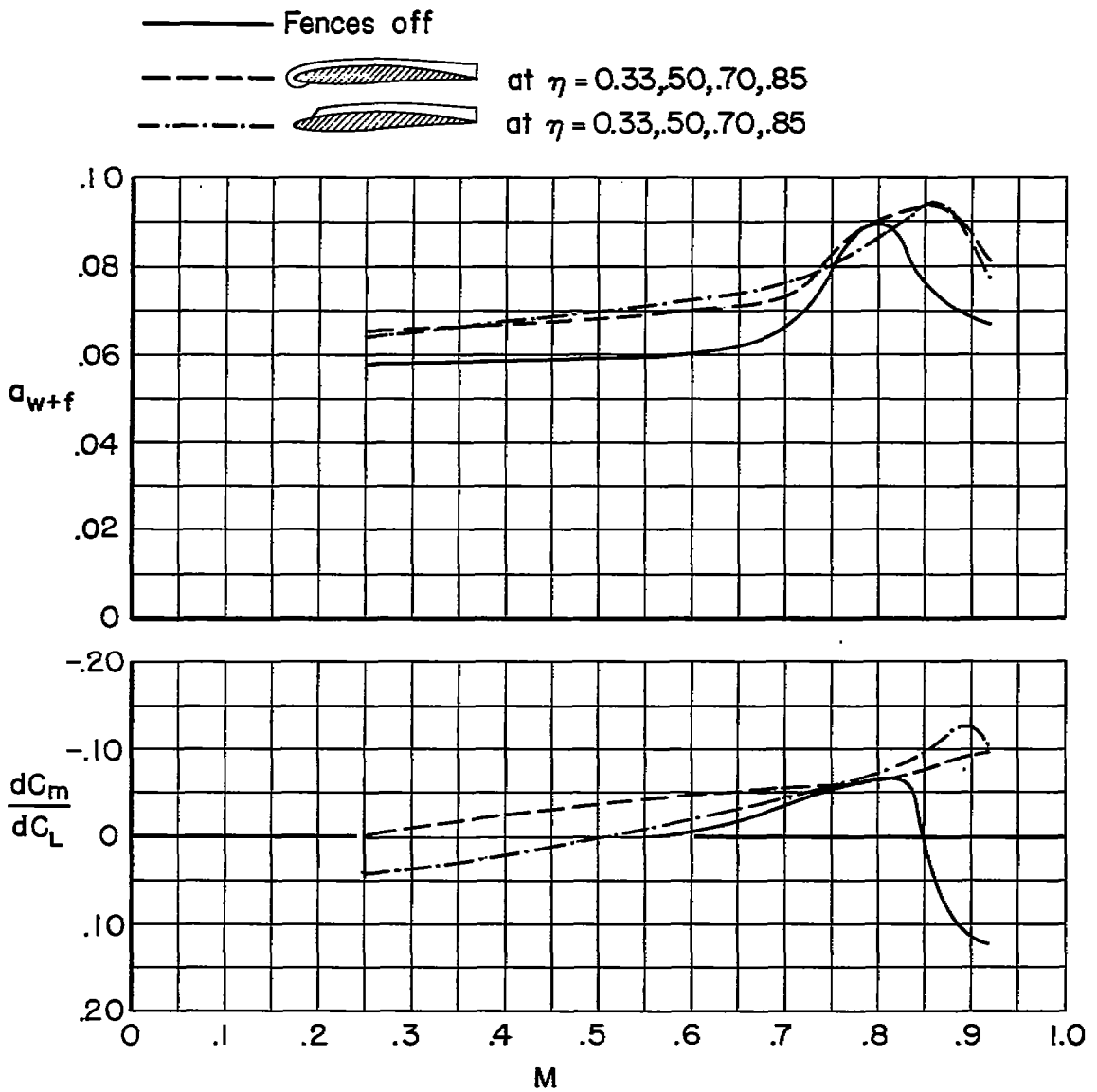

Figure 13.- The variation with Mach number of the slopes of the lift and pitching-moment curves of the wing-fuselage combination with and without wing fences: $C_L = 0.40$, R = 2,000,000.

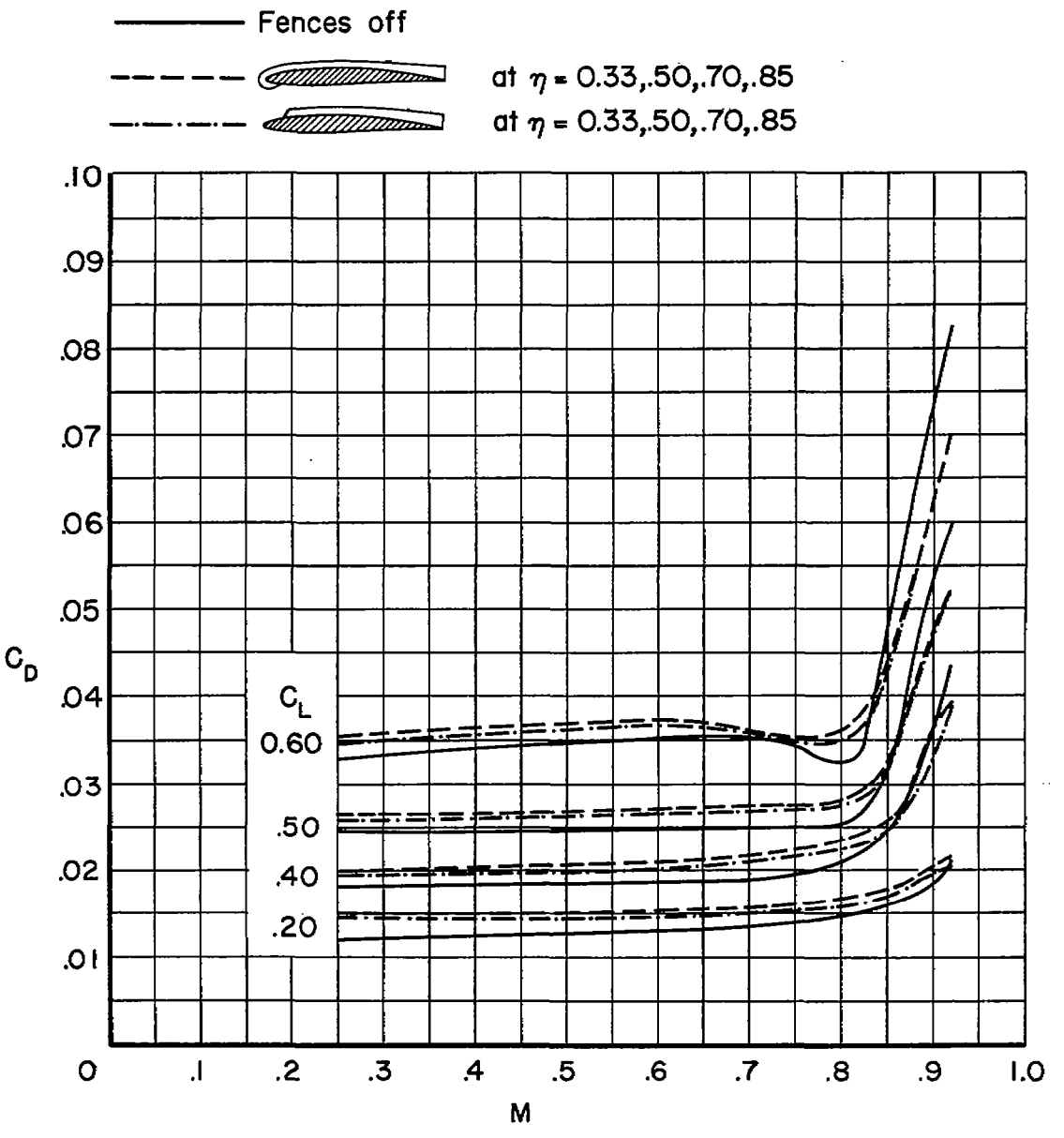

Figure 14.- The variation with Mach number of the drag coefficients of the wing-fuselage combination with and without wing fences at several constant lift coefficients; R = 2,000,000.

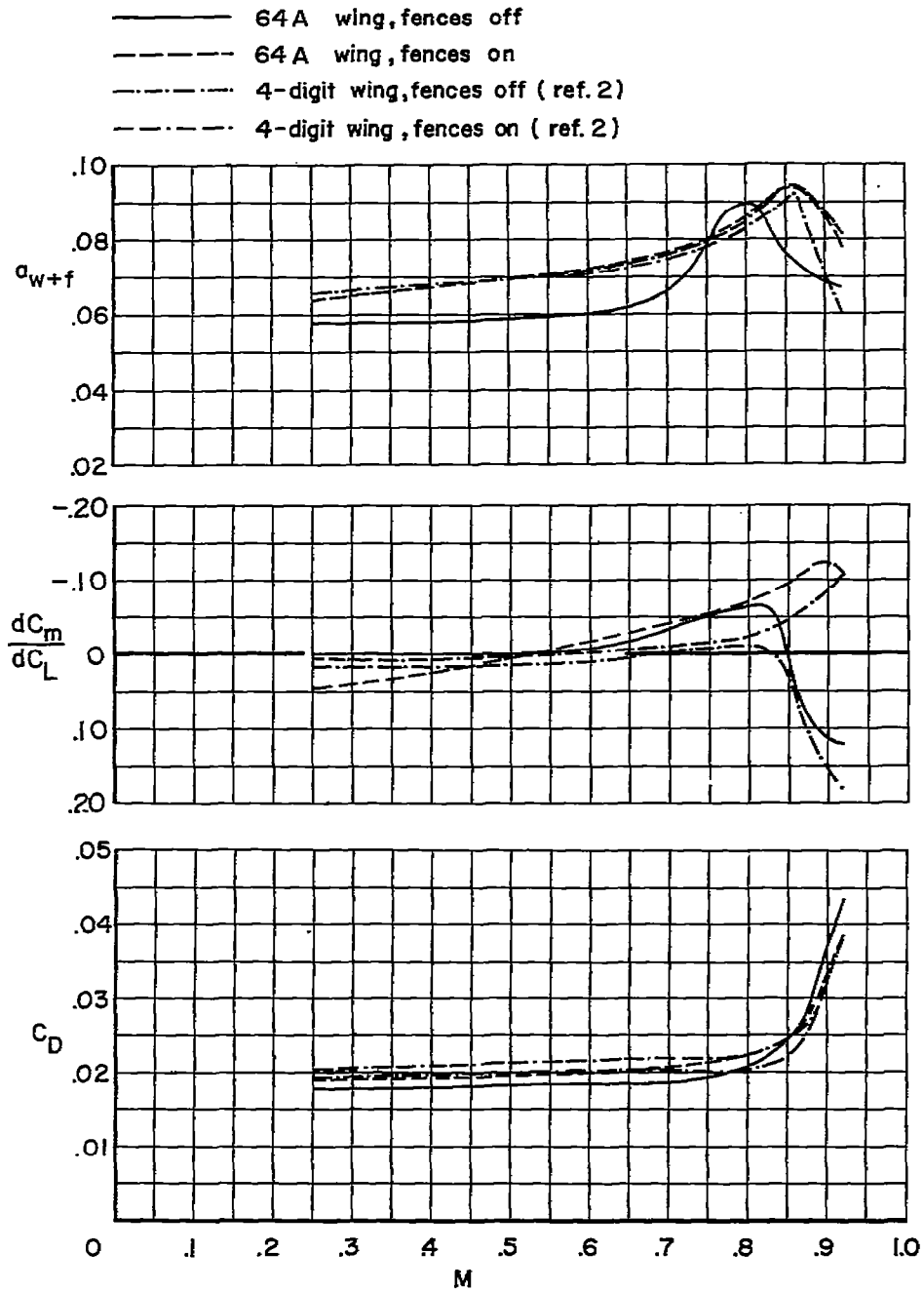

Figure 15.- Comparison of the longitudinal characteristics of the 64A and four-digit wing-fuselage combinations with and without partial-chord fences; C_L = 0.40, R = 2,000,000.

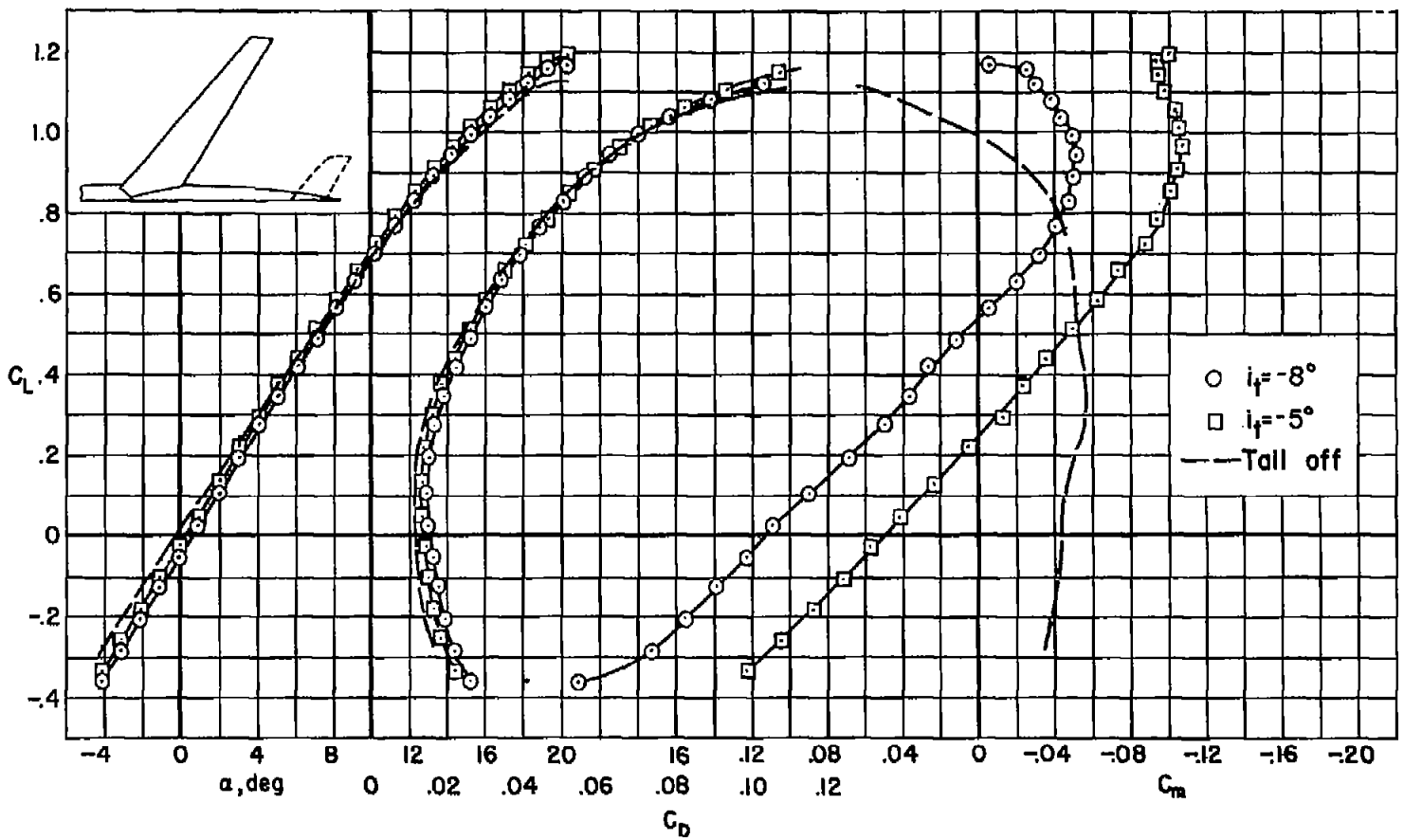

(a) M = 0.25, R = 8,000,000.

Figure 16.- The longitudinal characteristics of the combination with a horizontal tail; fences off.

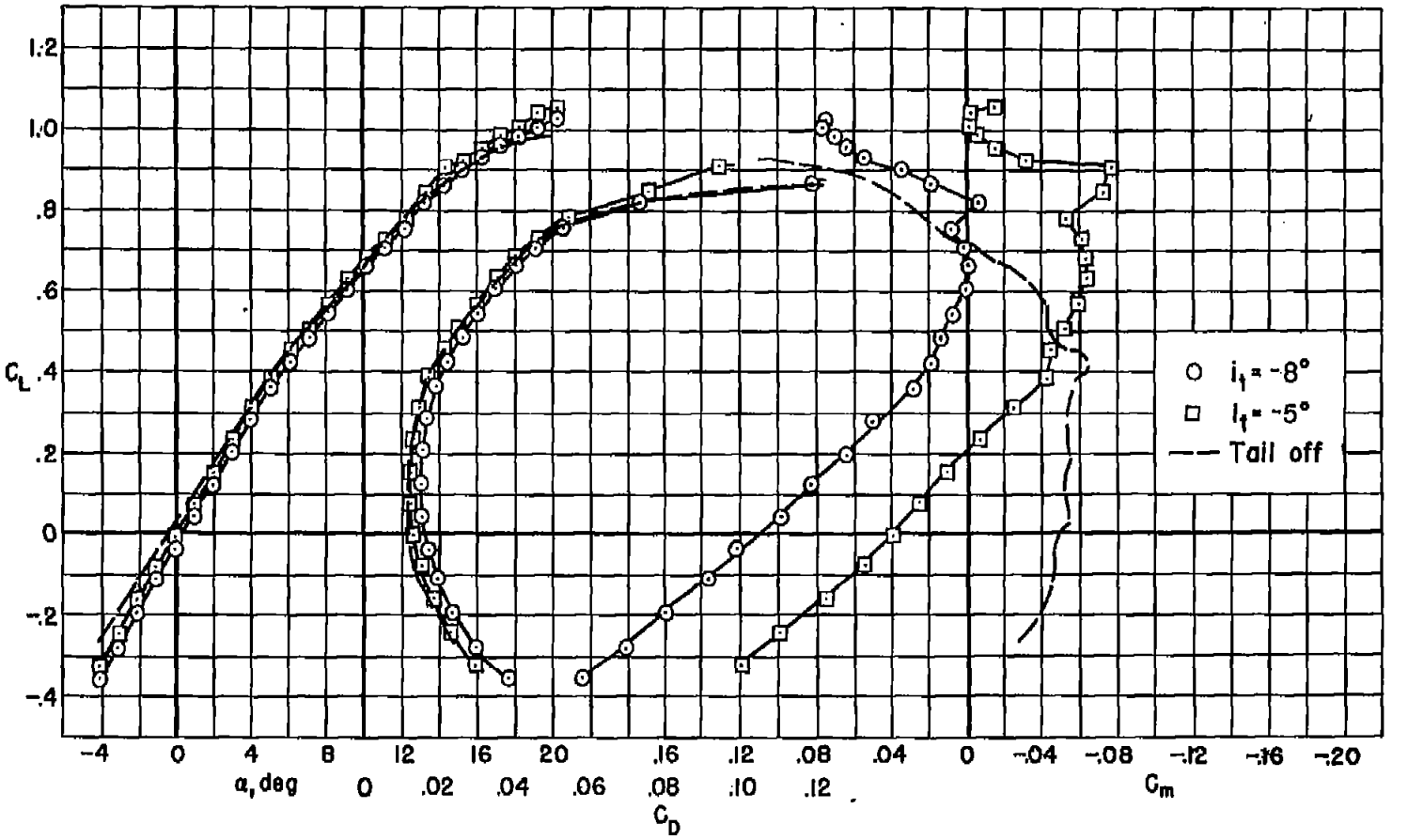

(b) M = 0.25, R = 2,000,000.

Figure 16.- Continued.

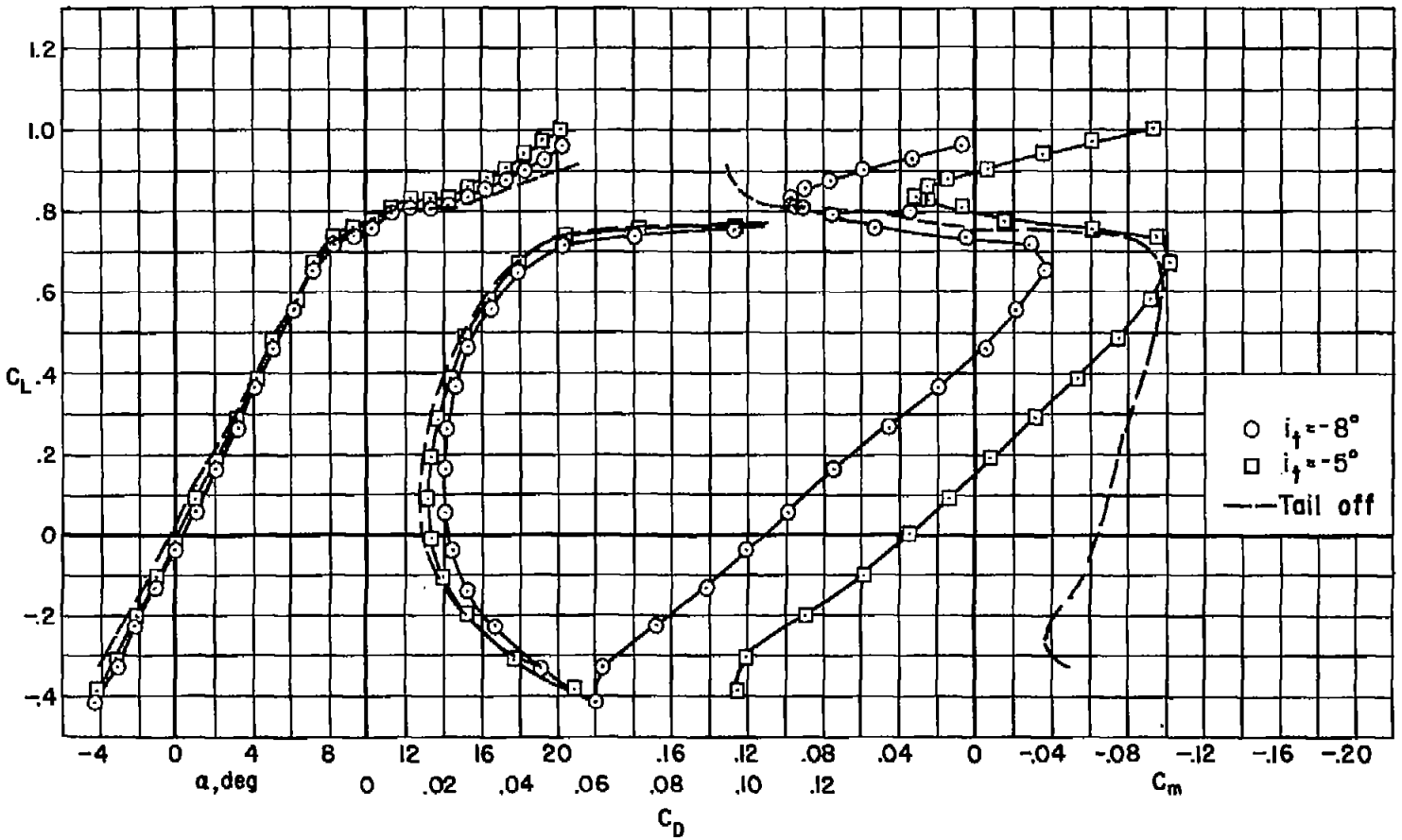

(c) M = 0.80, R = 2,000,000.

Figure 16.- Continued.

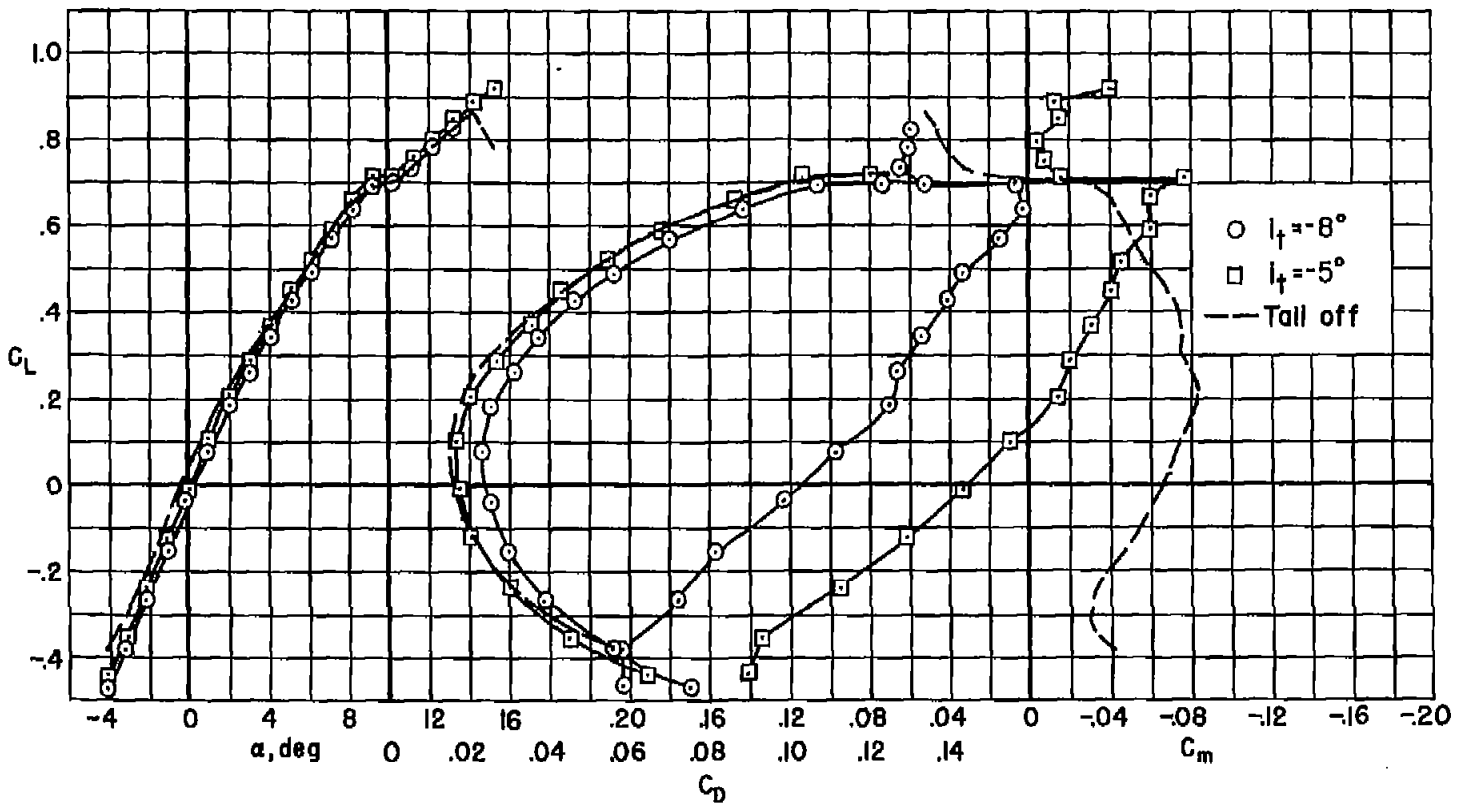

(d) M = 0.90, R = 2,000,000.

Figure 16.- Concluded.

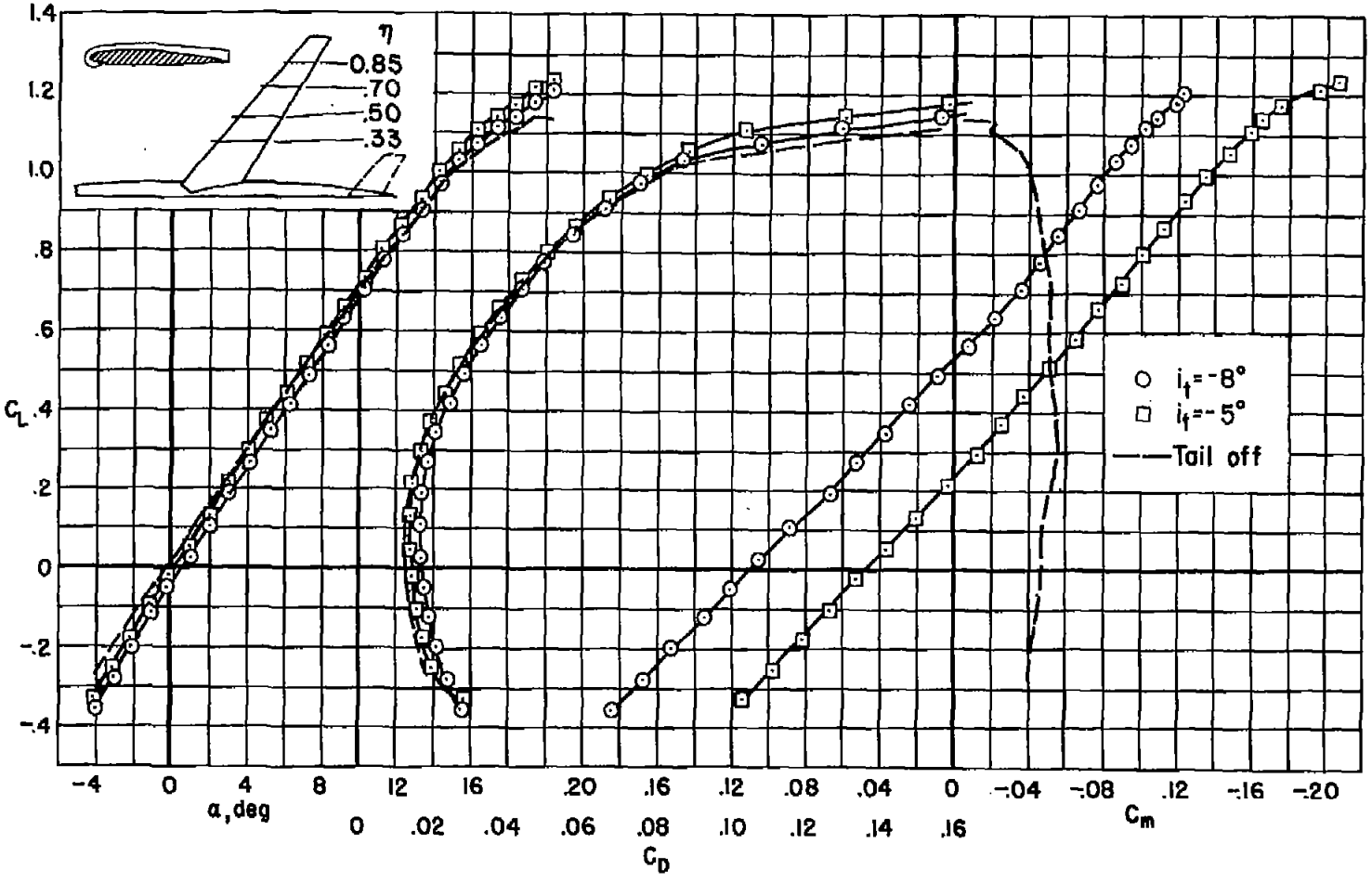

(a) M = 0.25, R = 8,000,000.

Figure 17.- The longitudinal characteristics of the combination with fences and a horizontal tail.

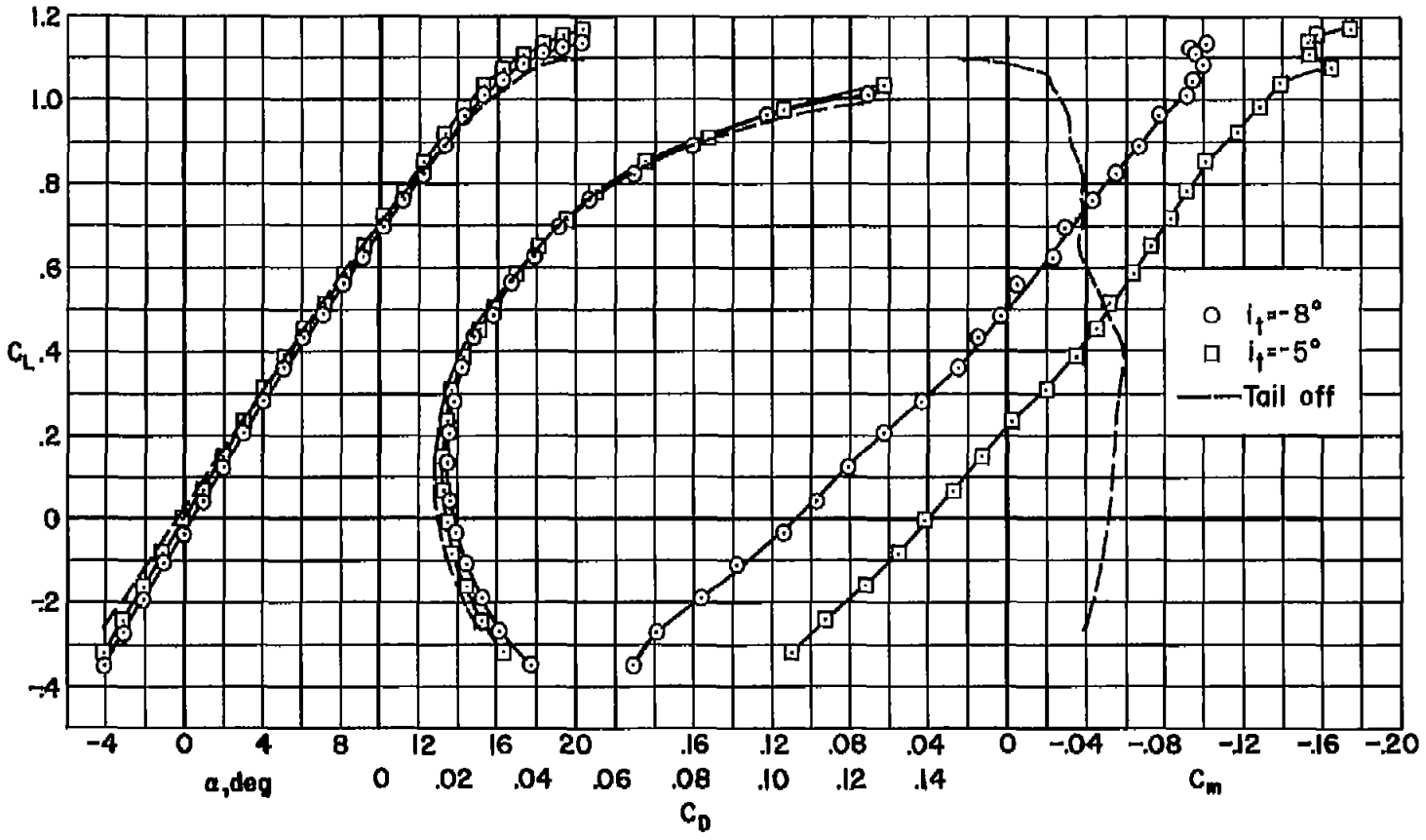

(b) M = 0.25, R = 2,000,000.

Figure 17.- Continued.

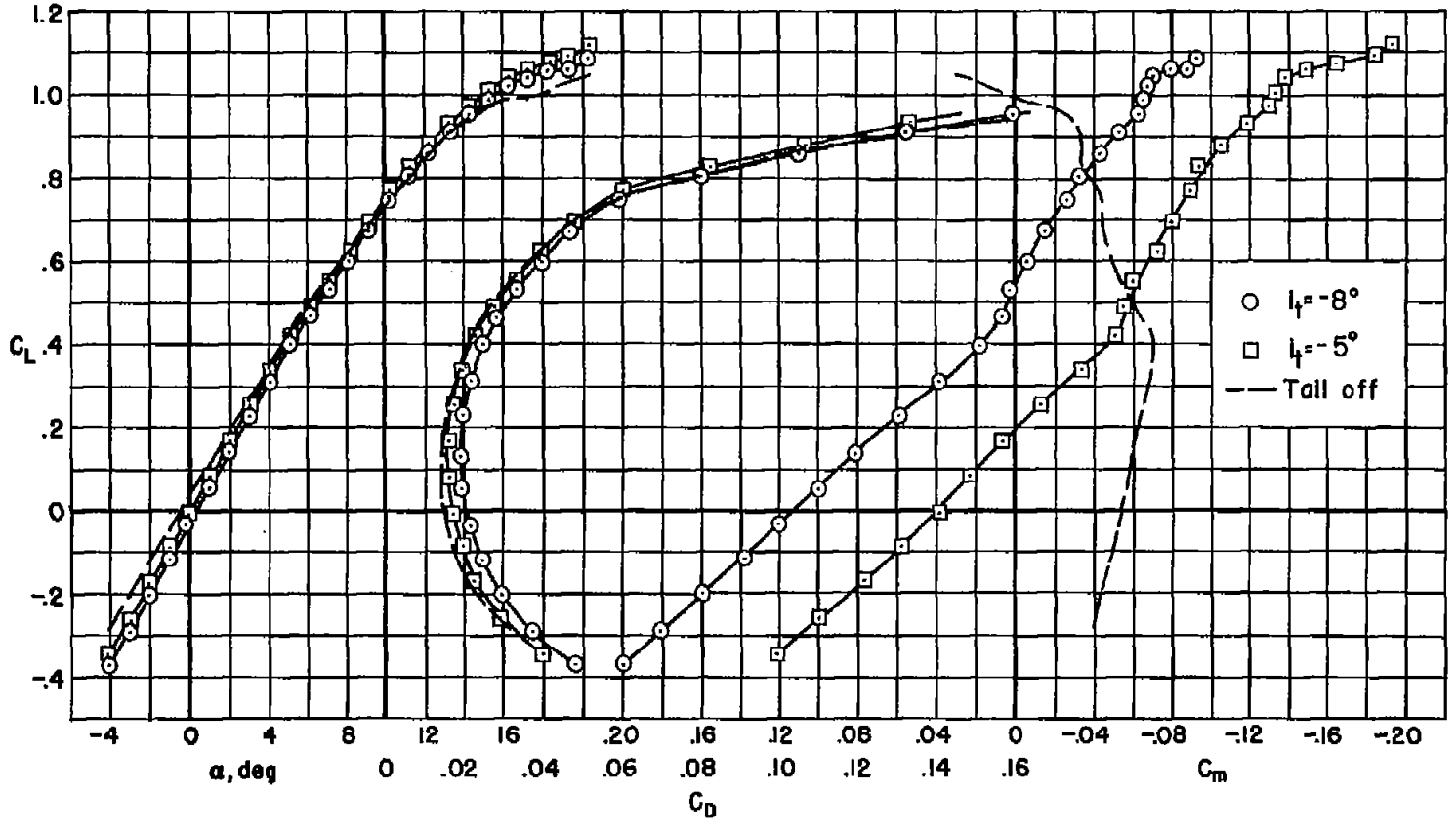

(c) M = 0.60, R = 2,000,000.

Figure 17.- Continued.

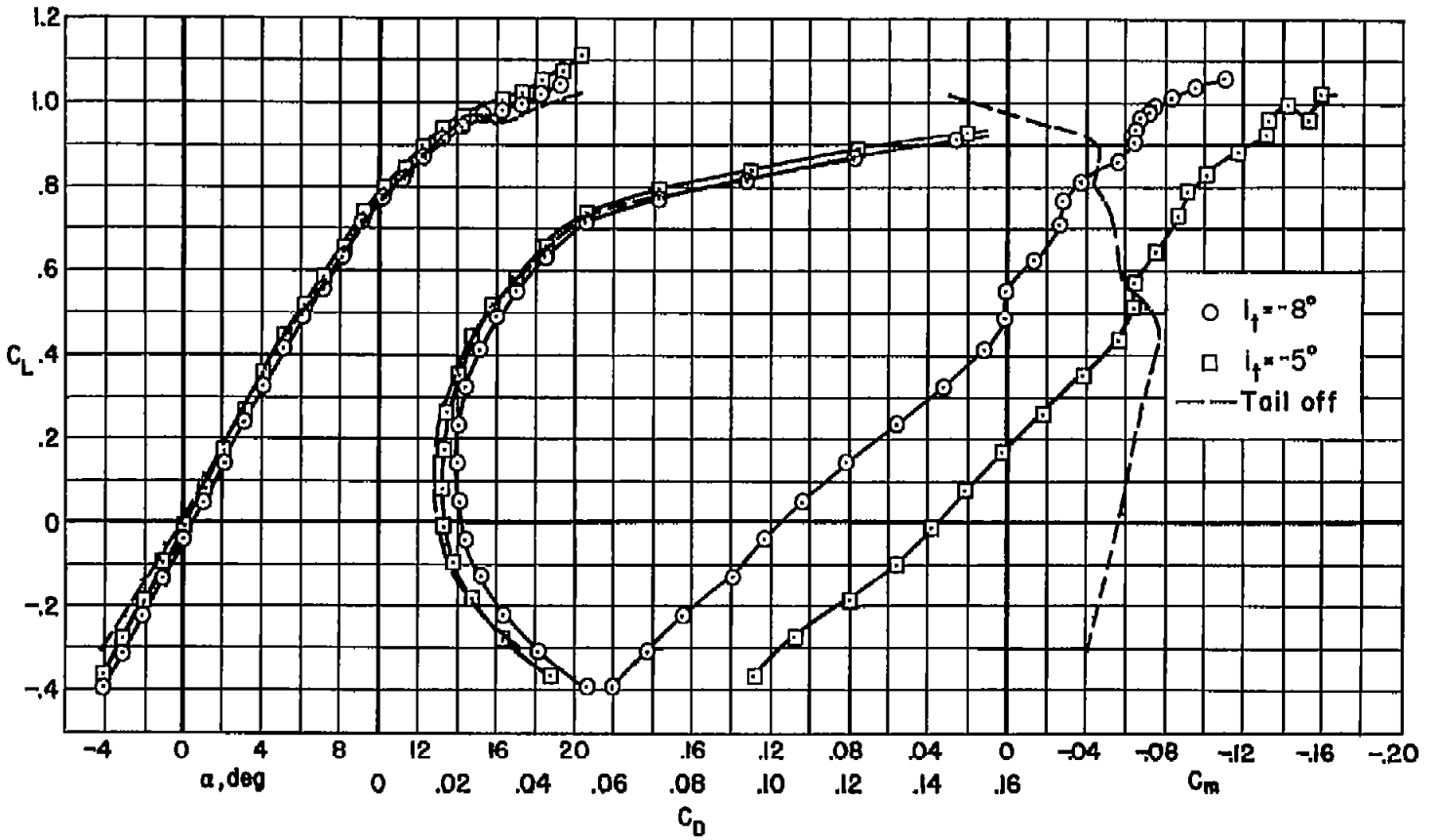

(d) M = 0.70, R = 2,000,000.

Figure 17.- Continued.

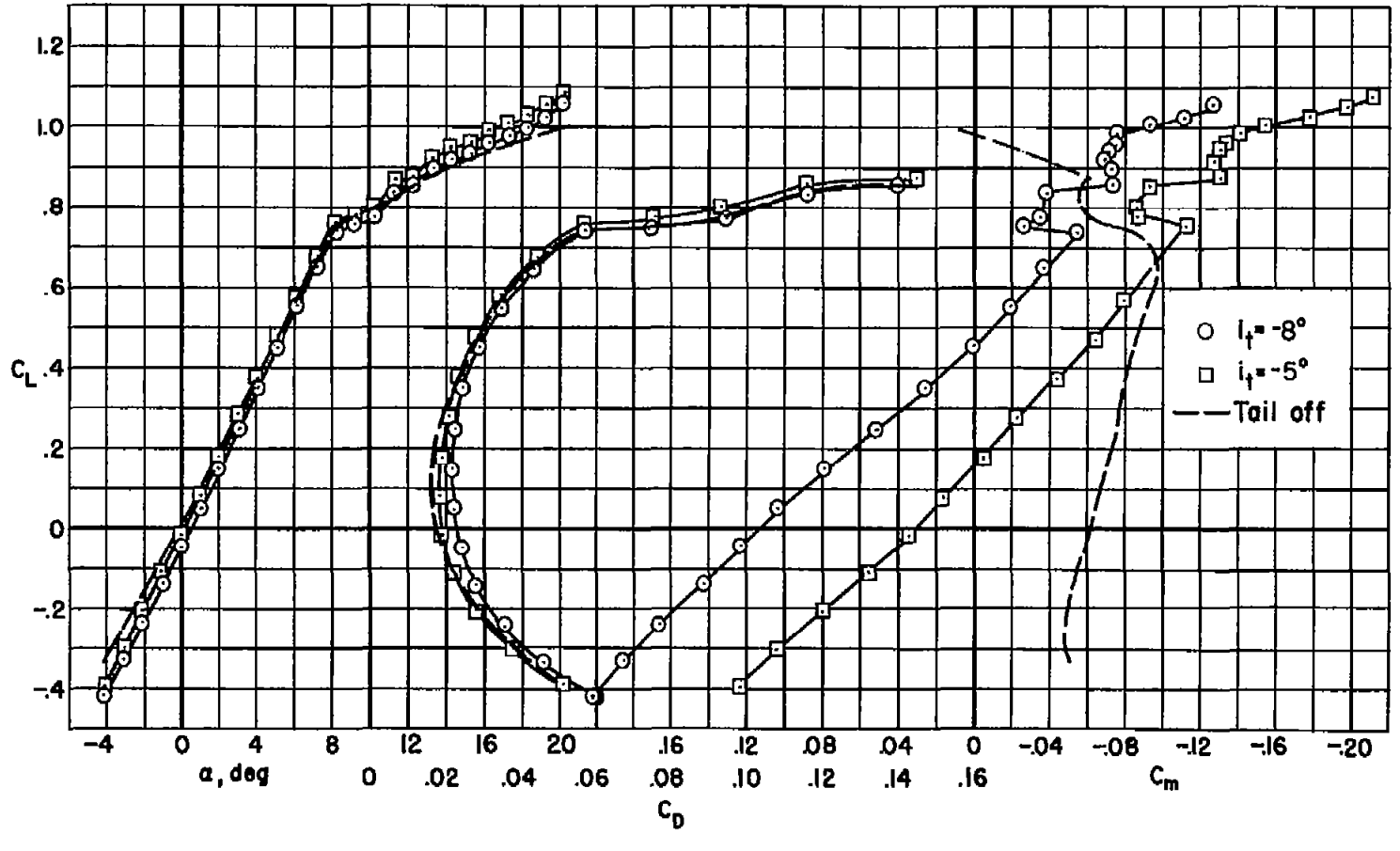

(e) M = 0.80, R = 2,000,000.

Figure 17.- Continued.

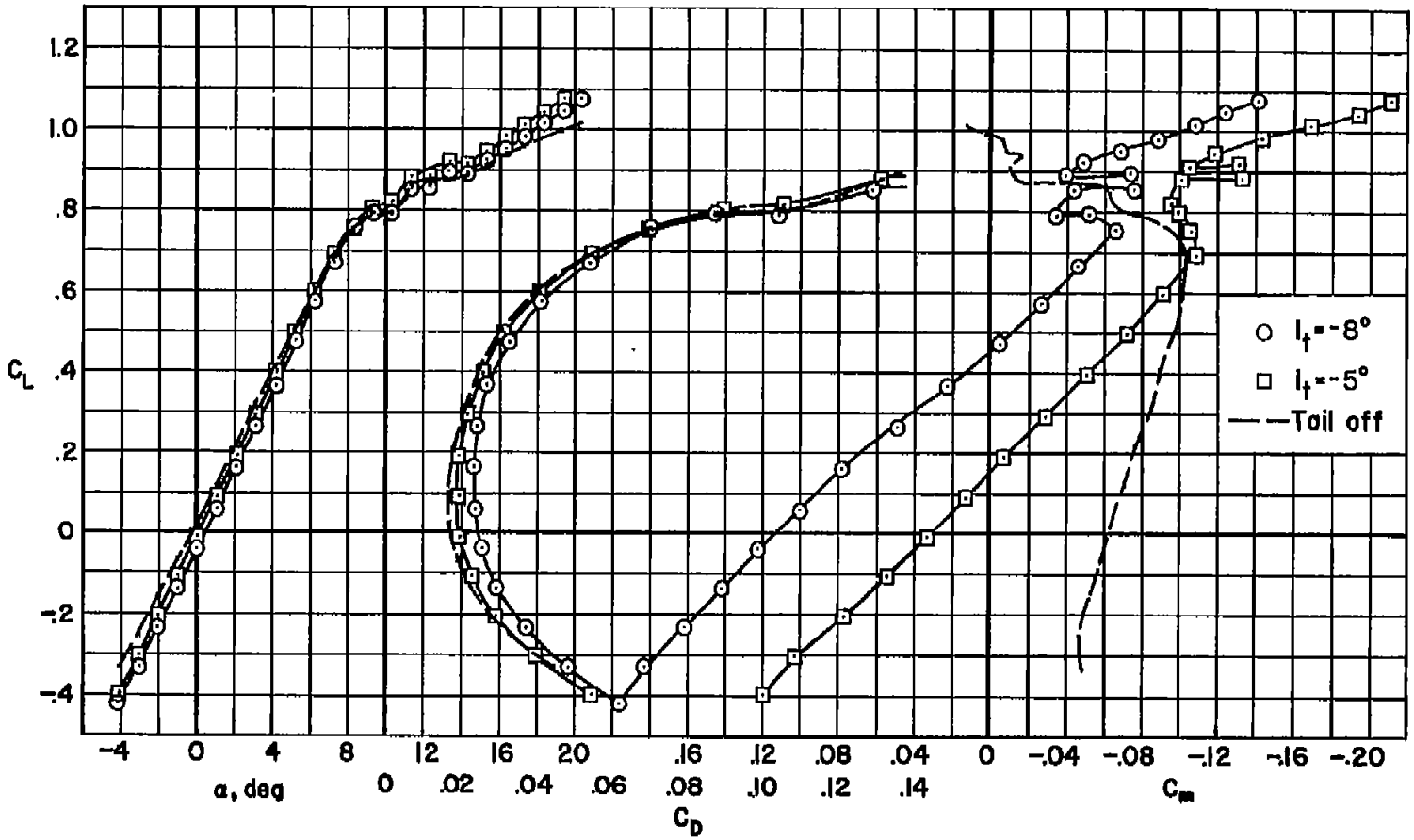

(f) M = 0.83, R = 2,000,000.

Figure 17.- Continued.

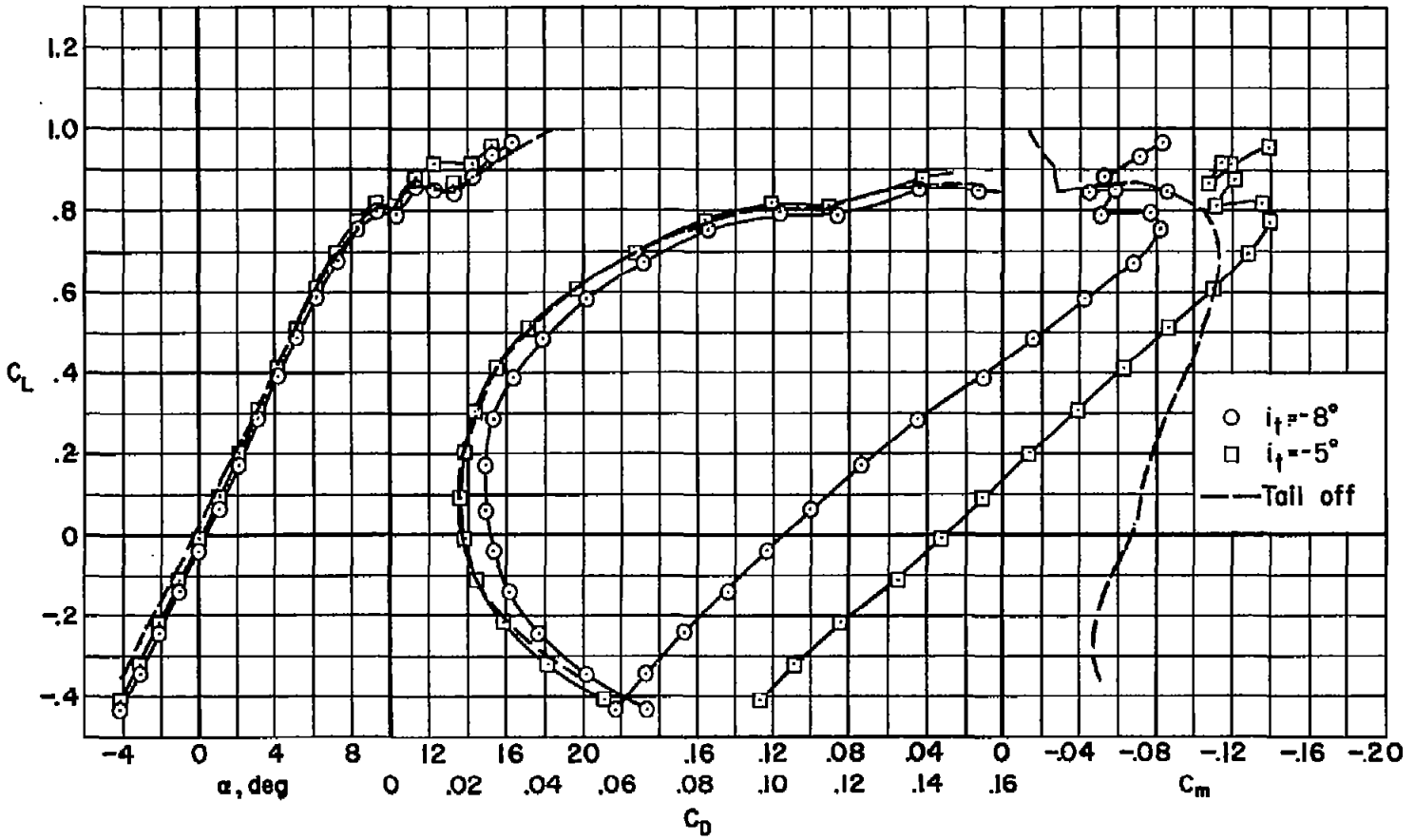

(g) M = 0.86, R = 2,000,000.

Figure 17.- Continued.

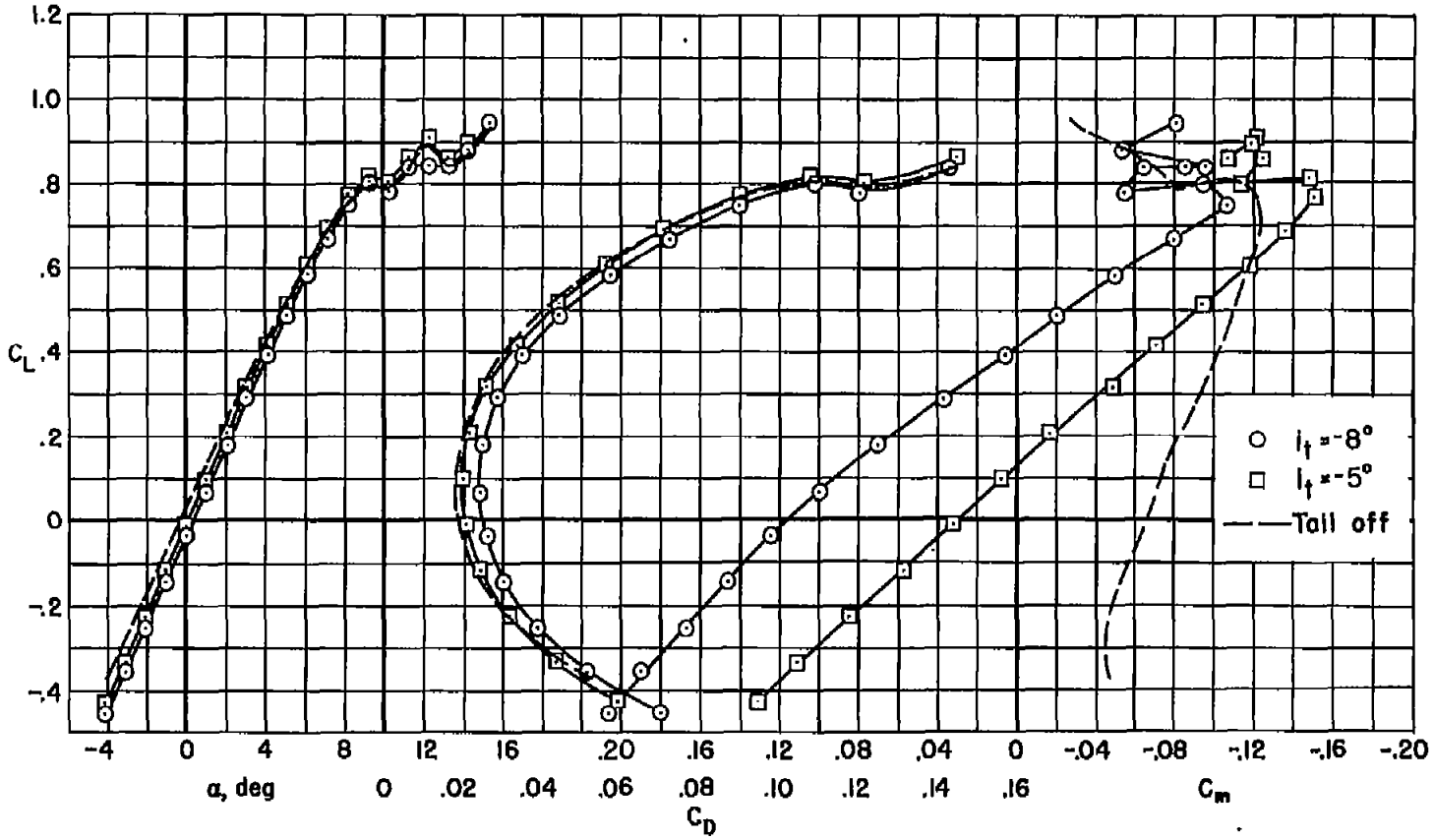

(h) M = 0.88, R = 2,000,000.

Figure 17.- Continued.

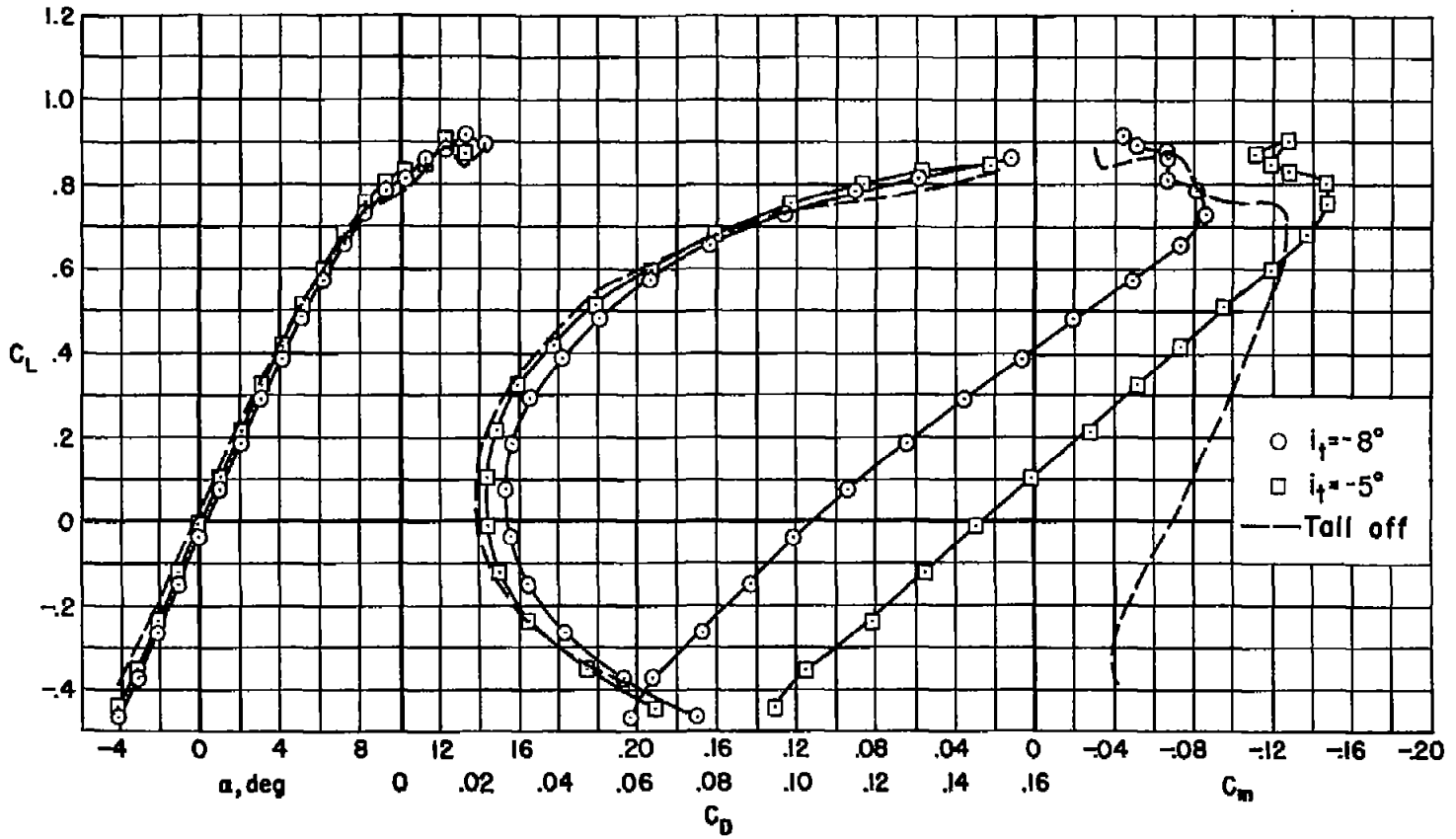

(i) M = 0.90, R = 2,000,000.

Figure 17.- Continued.

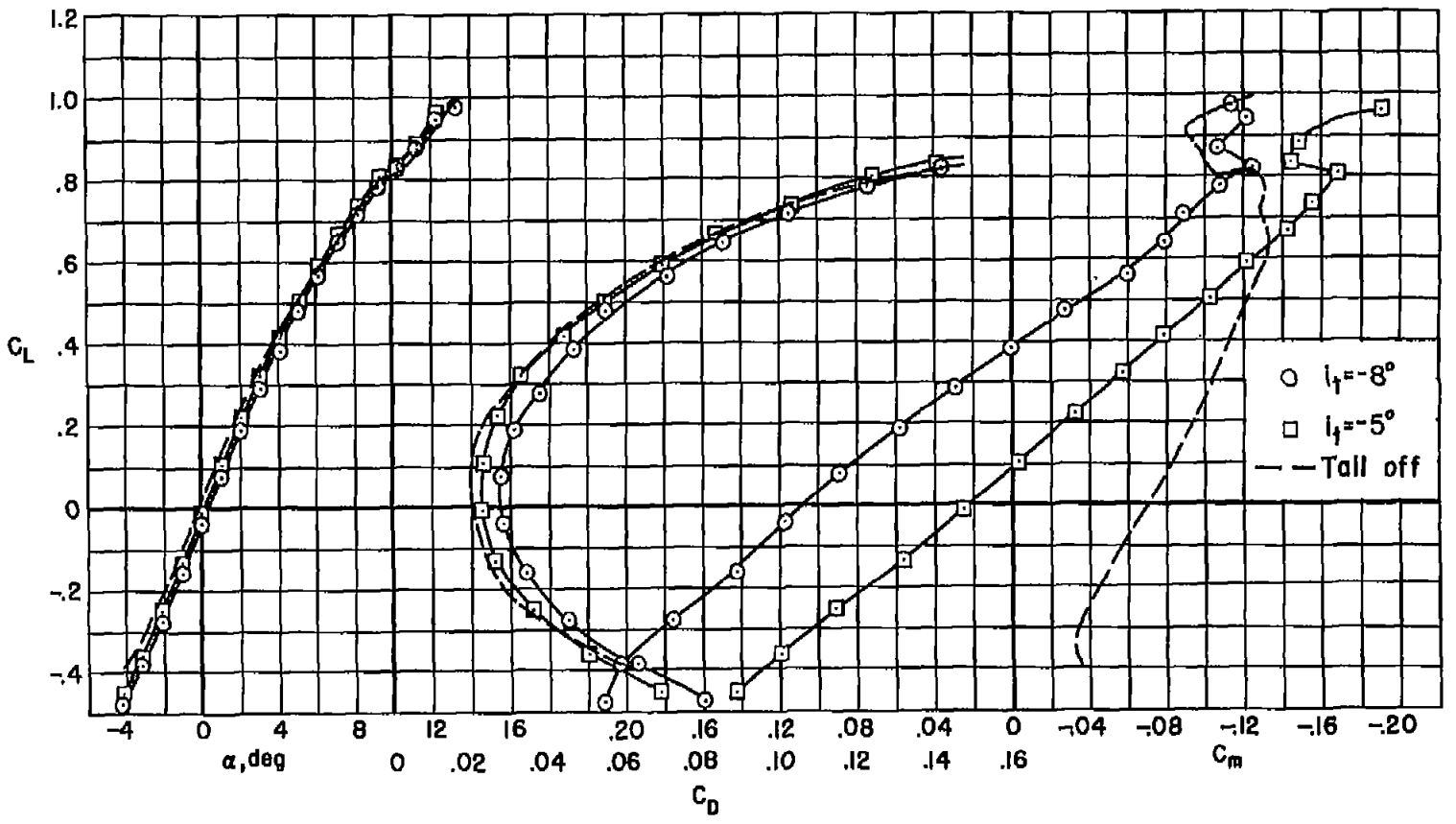

(j) M = 0.92, R = 2,000,000.

Figure 17.- Concluded.

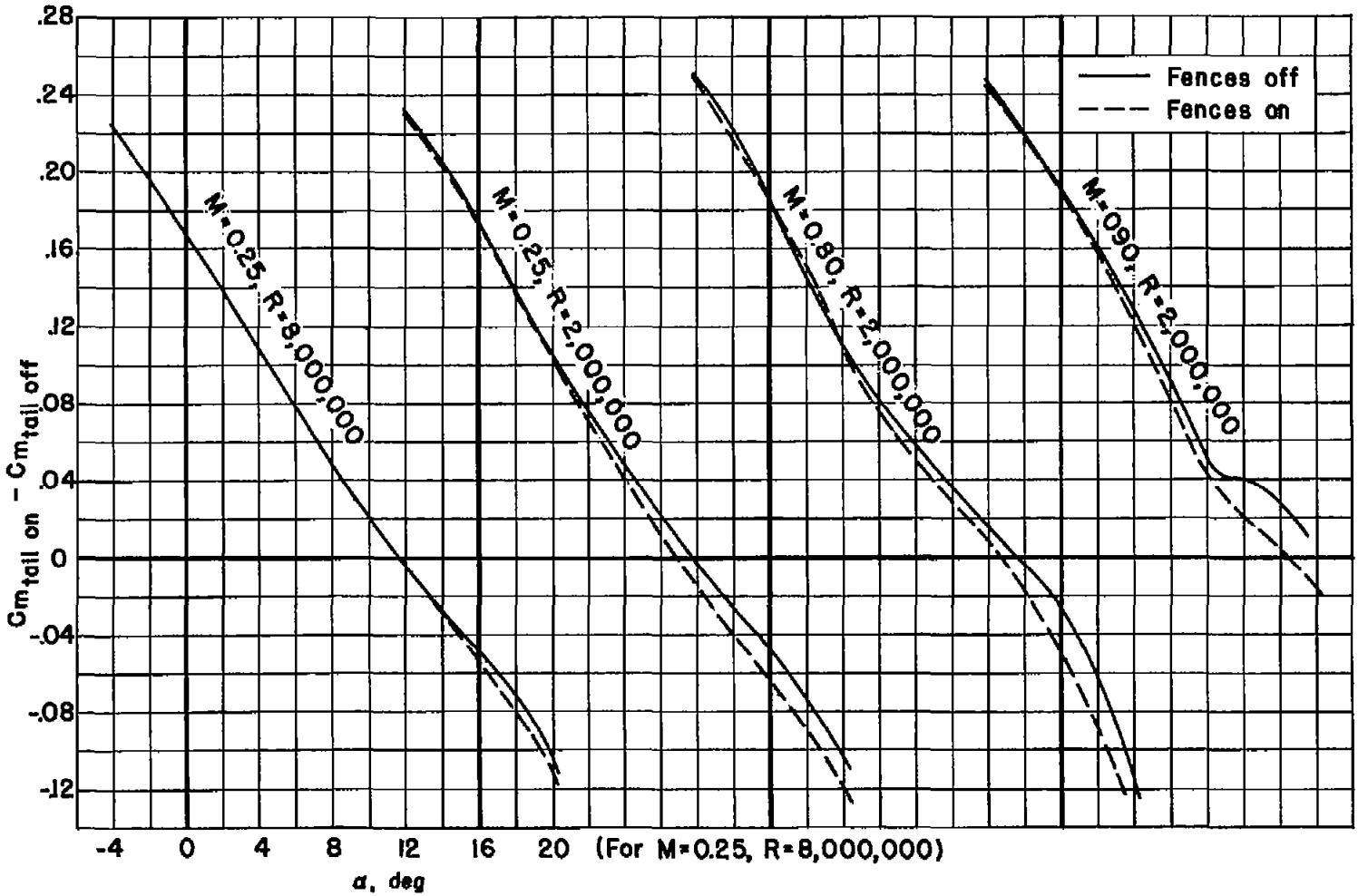

Figure 18.- Pitching-moment coefficient due to the horizontal tail: $i_t = -8^\circ$.

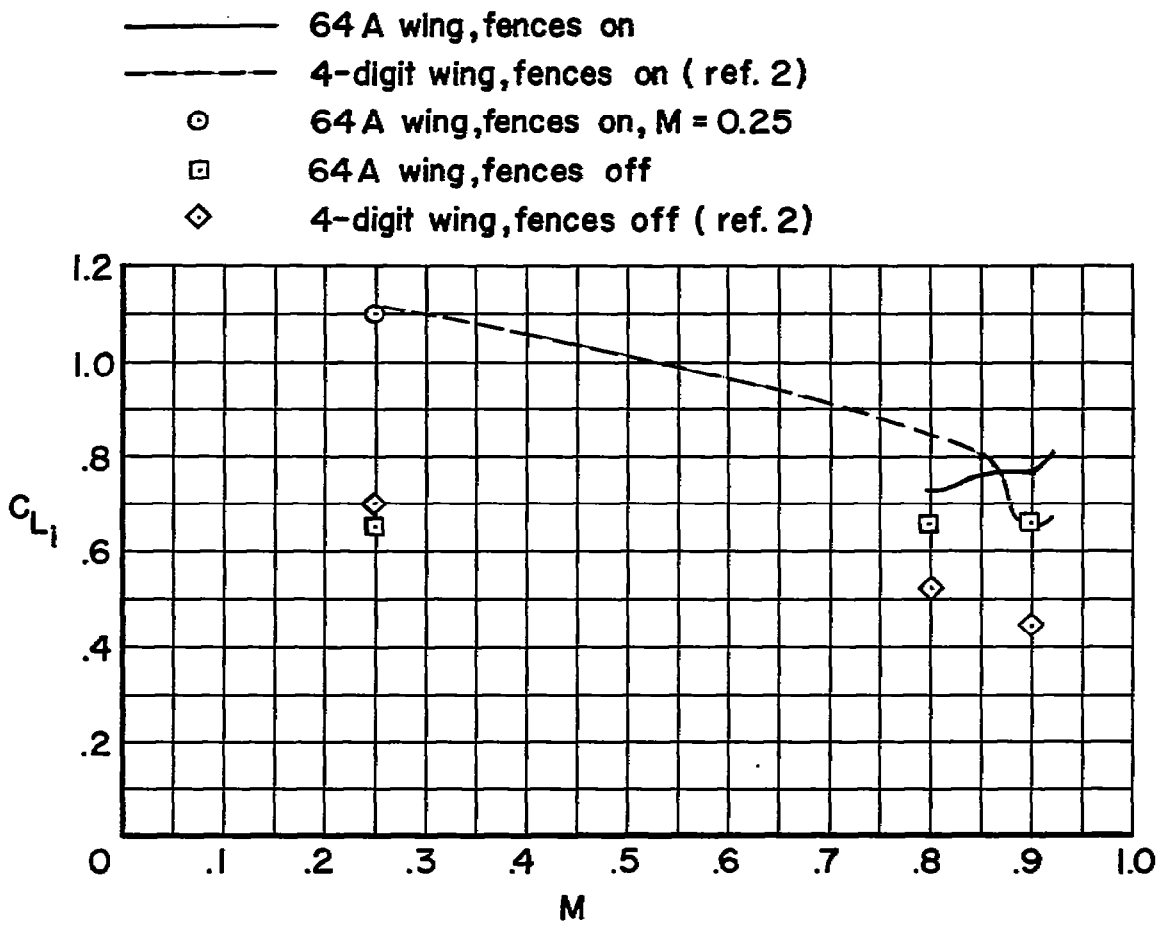

Figure 19.- The variations with Mach number of the inflection lift coefficients of the 64A and four-digit wing-fuselage-tail combinations with and without wing fences; $i_t = -8^\circ$, R = 2,000,000.

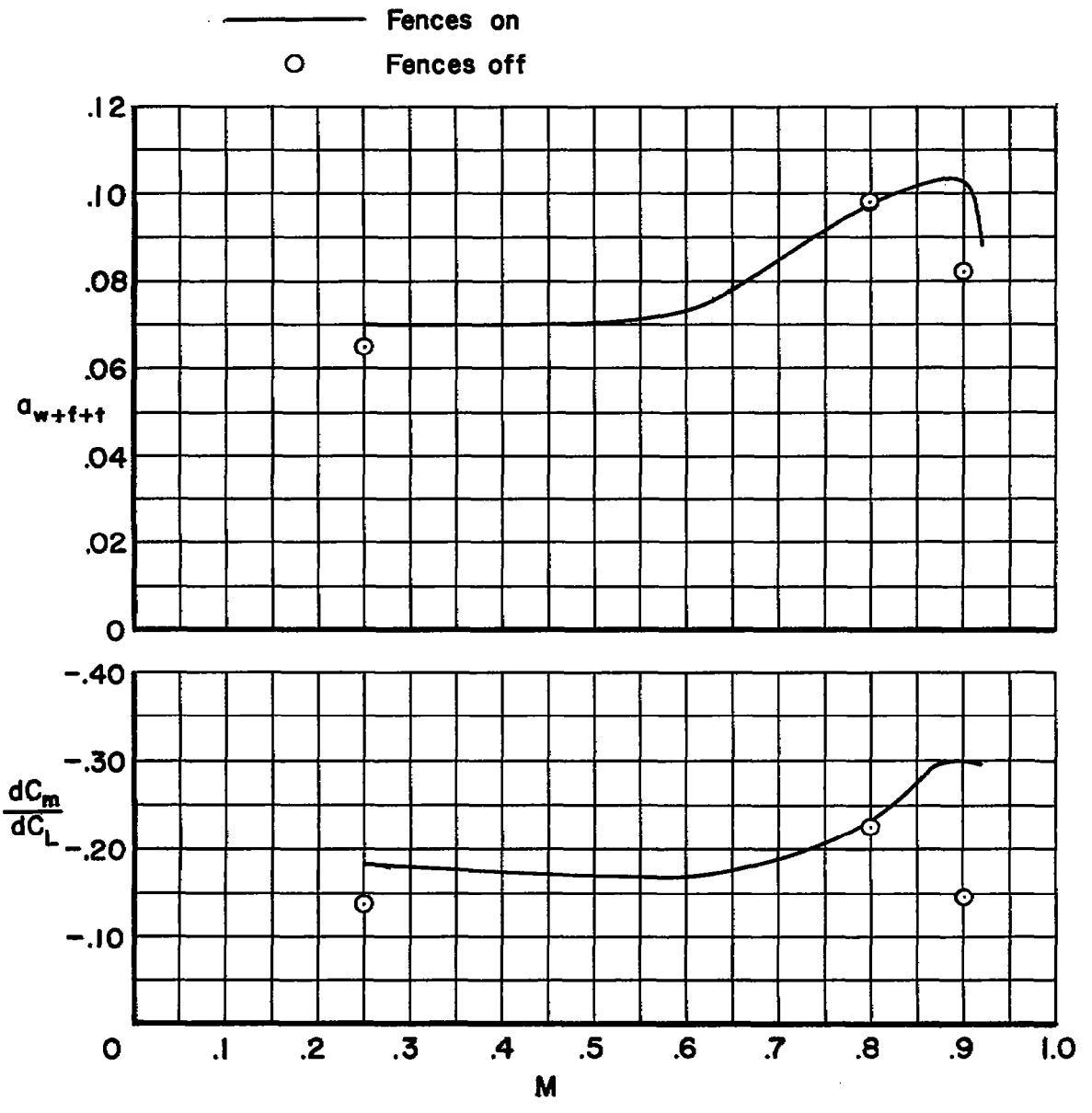

Figure 20.- The variations with Mach number of the slopes of the lift and pitching-moment curves of the wing-fuselage-tail combination with and without wing fences; $i_t = -8^\circ$, $C_L = 0.40$, $R = 2{,}000{,}000$.

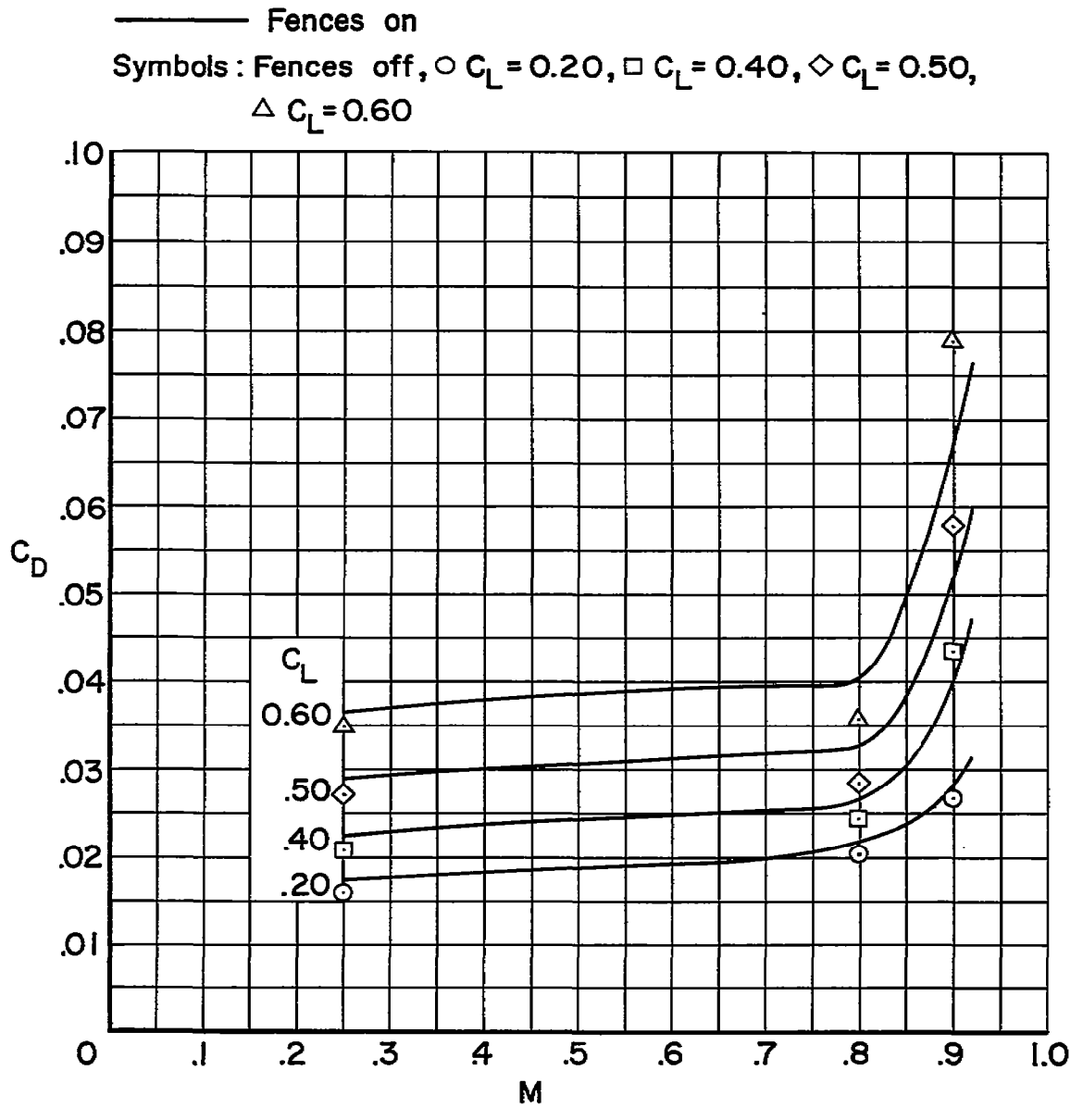

Figure 21.- The variation with Mach number of the drag coefficients of the wing-fuselage-tail combination with and without wing fences; $i_t = -8^\circ$, $C_L = 0.40$, $R = 2{,}000{,}000$.

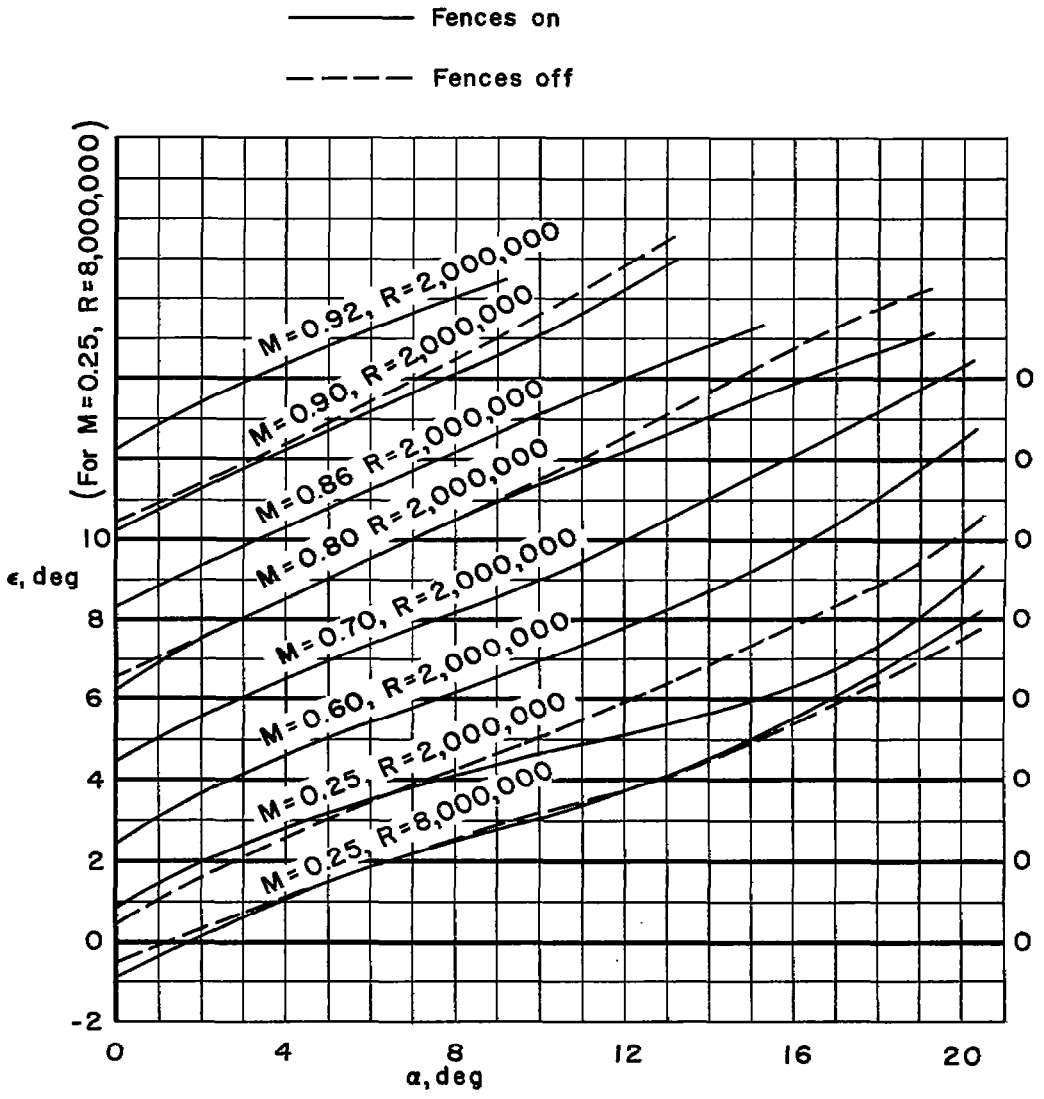

(a) ϵ vs. α.

Figure 22.- The variation with angle of attack of the factors affecting the stability contribution of the horizontal tail.

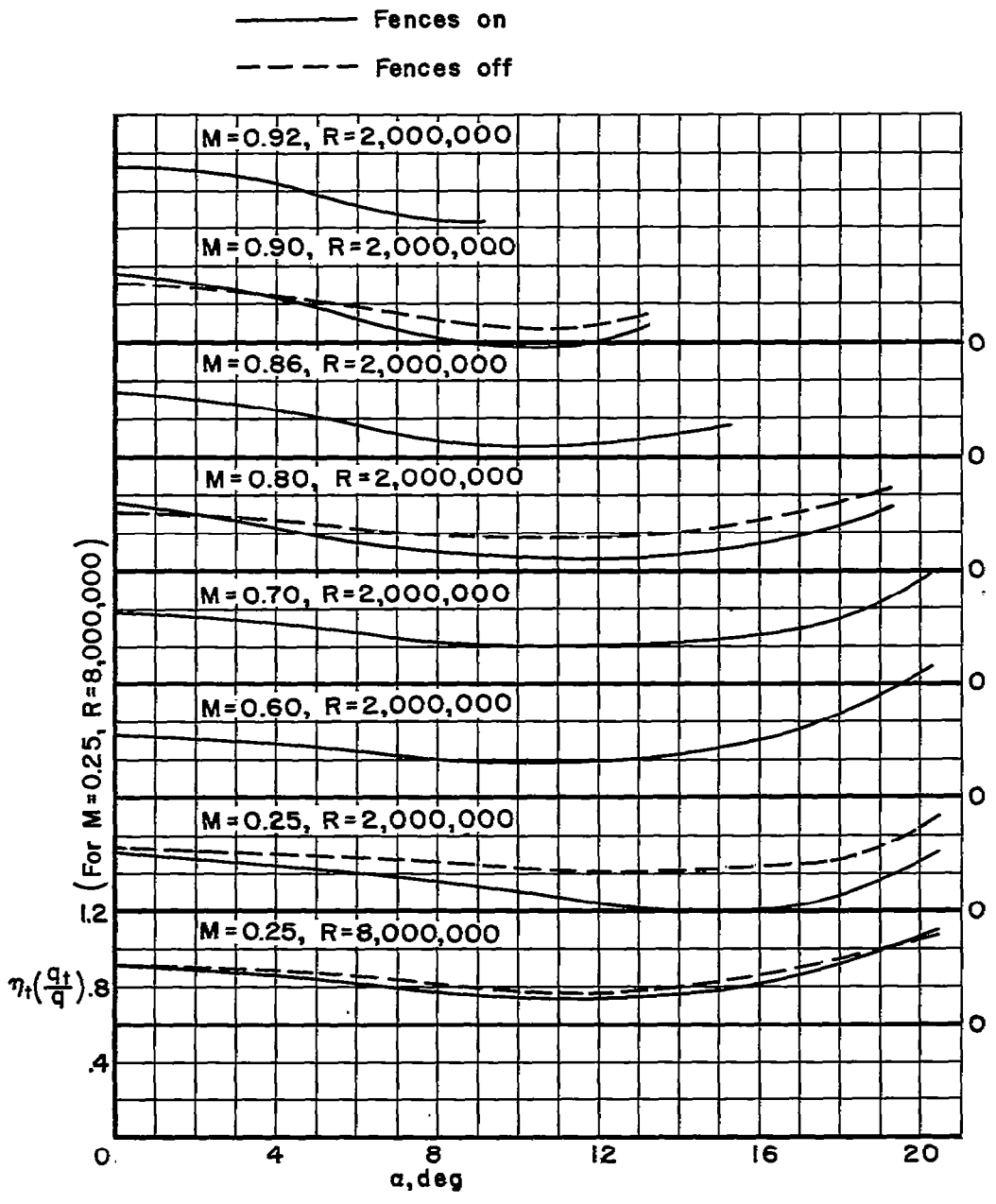

(b) $\eta_t(q_t/q)$ vs. α.

Figure 22.- Continued.

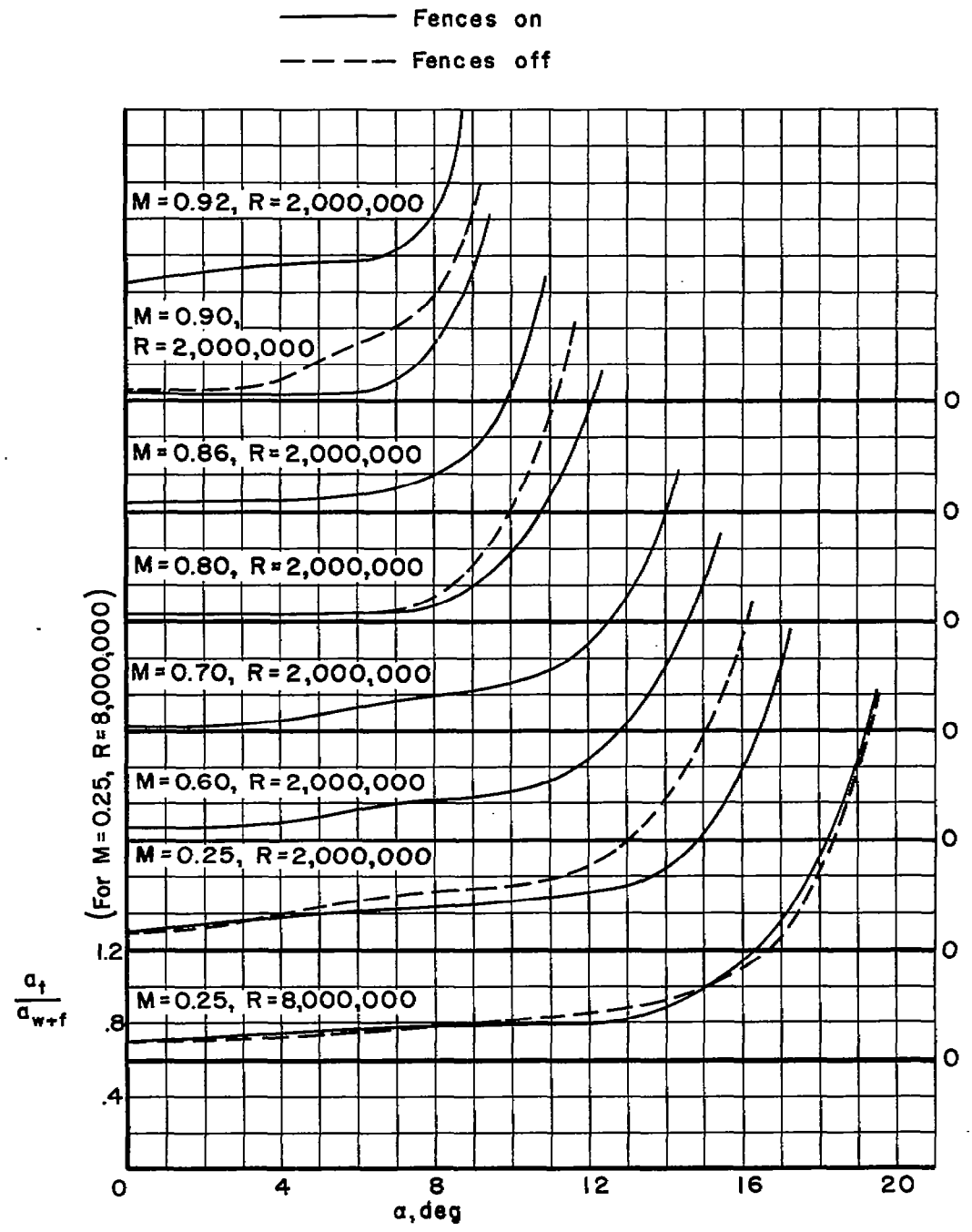

(c) a_t/a_{w+f} vs. α.

Figure 22.- Concluded.

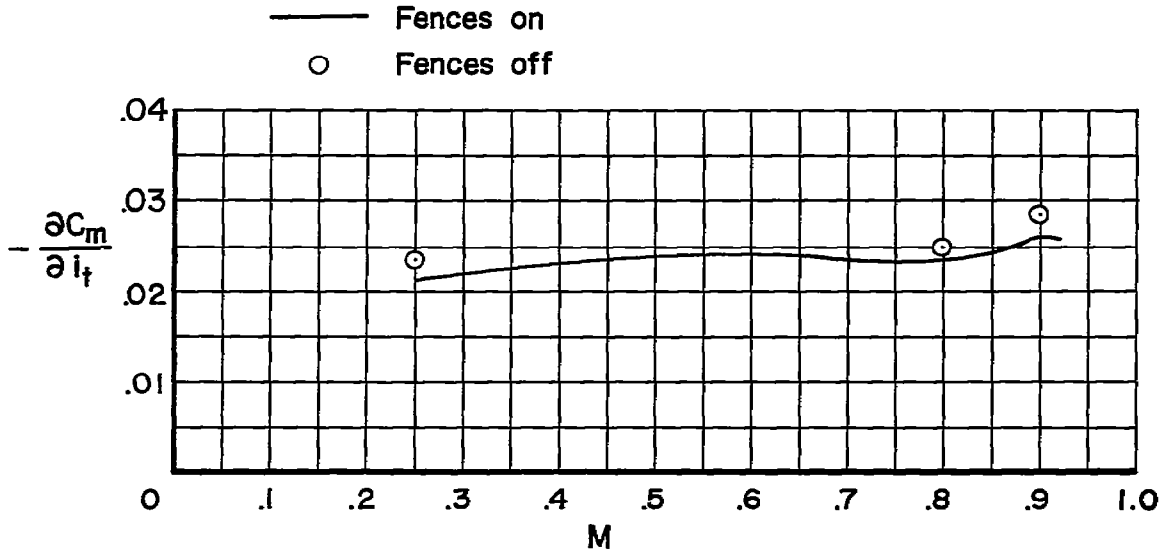

Figure 23.- The variation with Mach number of the control-effectiveness of the horizontal tail; $\alpha = 4^{\circ}$, R = 2,000,000.

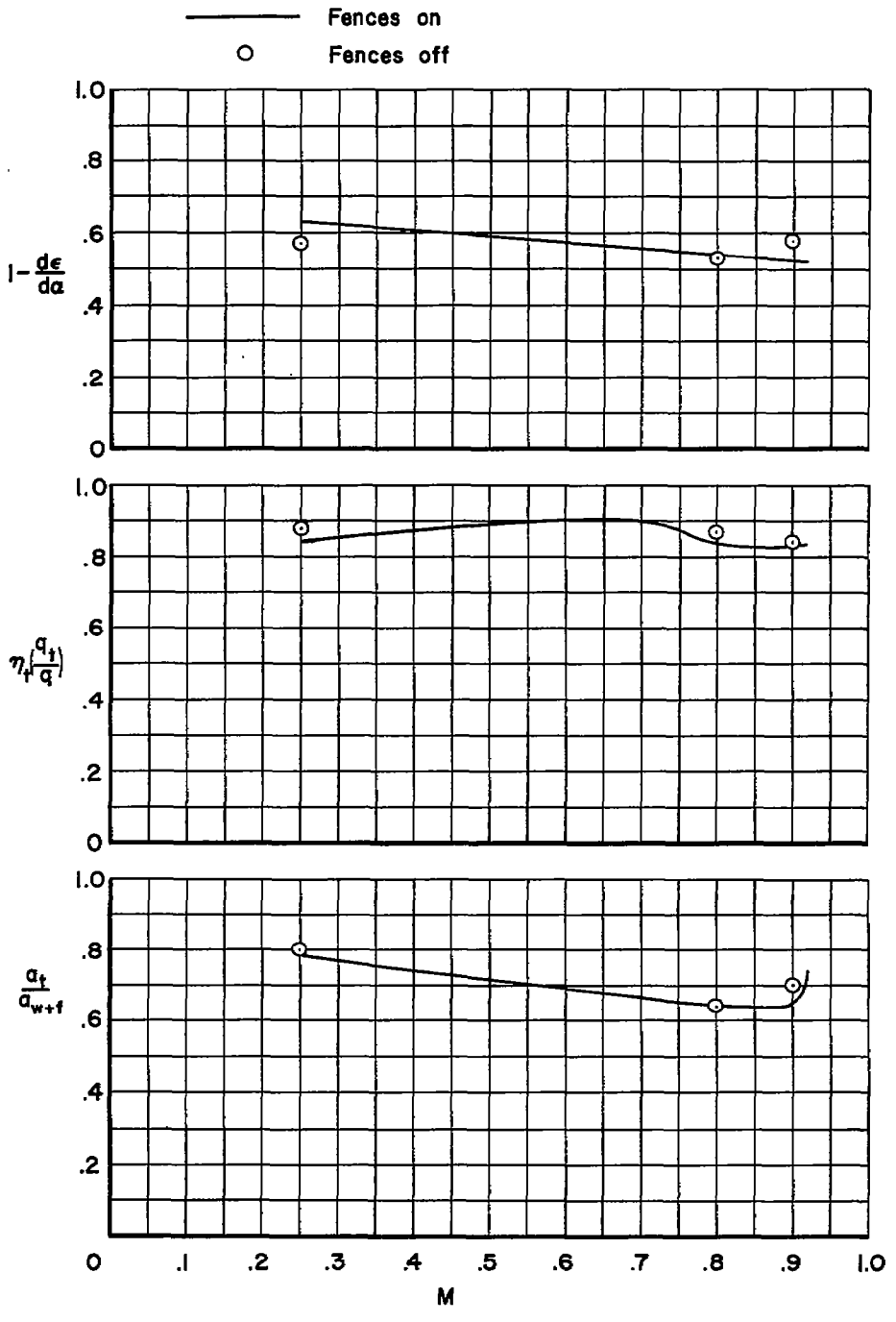

Figure 24.- The variation with Mach number of the factors affecting the stability contribution of the horizontal tail; $\alpha = 4^{\circ}$, R = 2,000,000.

NACA-Langley - 5-27-55 - 350